DEPARTMENT OF PEDIATRICS

ALBERT SZENT-GYÖRGYI MEDICAL AND PHARMACEUTICAL CENTER

UNIVERSITY OF SZEGED

MOLECULAR GENETIC MAPPING OF COSTELLO SNYDROME AND HEME OXYGENASE-1 GENE EXPRESSION STUDIES IN PEDIATRIC PATIENTS

ZOLTÁN MARÓTI

Ph.D. thesis

2004

ARTICLES RELATED TO THE THESIS

I. Maroti Z, Kutsche K, Sutajova M, Gal A, Nothwang HG, Czeizel AE, Timar L, Solyom E.: **Refinement and delineation of the breakpoint regions of a chromosome 1;22 translocation in a patient with Costello syndrome.**
Am J Med Genet. 2002 May 1;109(3):234-7.
PMID: 11977185

II. Zoltán Maróti*, Sándor Túri, Ilona Németh, Eszter Karg, Péter Ugocsai, Emőke Endreffy: **Heme oxygenase 1 (HMOX1) gene expression in hemodialysed uremic patients.**
Acta Biologica Szegediensis, 47(1-4):147-151, 2003

III. Maróti Z, Németh I, Túri S, Karg E, Ugocsai P, Endreffy E: **Heme oxygenase 1 expression in young uremic patients on hemodialysis.**
Pediatr Nephrol. 2004 Apr;19(4):426-31. Epub 2004 Feb 24.
PMID: 14986081

IV. Farkas Ildikó, Maróti Zoltán, Katona Márta dr., Orvos Hajnalka dr., Németh Ilona dr., Endreffy Emőke dr., Pál Attila dr., Túri Sándor dr.: **Hemoxigenáz-1 génexpresszió érett és koraszülött újszülöttekben**
Magyar Nőorvosok Lapja [in press]

LIST OF ABBREVIATIONS

ADMA	asymmetric dimethylarginine
BAC	bacterial artificial chromosome
Bi	bilirubin
CDS	coding sequence
CRP	C-reactive protein
cDNA	complement DNA
cRT-PCR	competitive reverse-transcriptase PCR
DNA	deoxyribonucleic acid
ESRD	end-stage renal disease
EPO	erythropoietin
FISH	fluorescence *in situ* hybridization
FOX	ferroxidase
GSH	reduced glutathione
GSSG	oxidized glutathione
HD	hemodialysis
Hb	hemoglobin
HMOX1	heme oxygenase-1 gene
HMOX2	heme oxygenase-2 gene
HO-1	heme oxygenase-1 protein
HPLC	high pressure liquid chromatography
NF2	neurofibromatosis type 2
PAC	P1 artificial chromosome
PDGFB	platelet derived growth factor B
PCR	polymerase chain reaction
PTPN11	protein-tyrosine phospatase, nonreceptor-type 11
RNA	ribonucleic acid
STR	short tandem repeat
YAC	yeast artificial chromosome

ELECTRONIC DATABASES AND RESOURCES

NCBI	http://www.ncbi.nlm.nih.gov
BLAST	http://www.ncbi.nlm.nih.gov/BLAST/
RepeatMasker	http://ftp.genome.washington.edu/cgi-bin/RepeatMasker

Costello syndrome (OMIM no. 218040); PDGFB (GDB no. 120709); Neurofibromatosis type 2 (OMIN no. 101000); NF2 (GDB no. 120232); NT-026949 (GenBank no. 15295304); NT-011520 (Gen- Bank no. 15319019)
Heme oxygenase 1 (OMIM no. 141250); HMOX1 (GeneBank no. 47678540); HO-1 (GeneBank no. 16306631)

TABLE OF CONTENTS

1. INTRODUCTION

1.1. Costello syndrome

Costello syndrome (OMIM 218040; Faciocutaneoskeletal syndrome; FCS syndrome) is a rare congenital disorder characterized by postnatal growth deficiency, mental retardation, "coarse" face, loose skin of the neck, hands, and feet, cardiomyopathy, and nasal papillomata. The first cases were described in 1971 and 1977 [1, 2]. To date, the genetic basis of Costello syndrome is unknown. Autosomal dominant inheritence with de novo mutations has been suggested by Lurie [3] to explain the usually sporadic occurrence of the syndrome.

The hypothesis of autosomal recessive inheritance of Costello syndrome was based on 2 families with affected sibs [4, 5] and 2 consanguineous matings [3, 6]. Lurie [3] reviewed 20 reported families and found that the 37 sibs of probands were all normal. In 6 families for whom pedigrees were not available, 2 affected sib-pairs were born. Even if there were no normal offspring in these latter families, the occurrence of the Costello syndrome in only 2 of 39 sibs virtually excludes an autosomal recessive inheritance pattern ($P = 0.999$). Moreover, a significant increase of mean paternal age (38.0 years) and paternal-maternal age difference (7.36 years) suggests sporadic autosomal dominant mutations as a likely cause. The 2 reported cases of affected sibs born to healthy parents may be explained by germline mosaicism, although heterogeneity with a small proportion of recessively inherited cases cannot be excluded. In line with this hypothesis, advanced paternal age has been also found in the families analyzed by Johnson et al. [7]. The putative male to male transmission of Costello syndrome is also consistent with an autosomal dominant inheritance.

Because of phenotypic overlap between Costello syndrome and Noonan syndrome, and because mutations in the PTPN11 gene had been demonstrated in the latter, Tartaglia et al. [8] screened a cohort of 27 patients with clinically diagnosed Costello syndrome for PTPN11 mutations; they found none. The exclusion of PTPN11 mutations in cardiofaciocutaneous syndrome by Ion et al. [9] indicates that these 3 syndromes are distinct. A first clue to map the gene was provided by a Costello patient carrying an apparently balanced chromosomal translocation t(1;22) (q25;q11) [10].

1.2. Oxidative stress in neonates

Birth itself causes mechanical and oxidative stress for newborns. All infants, regardless of gestational age, have shown evidence of oxidative stress during the first few days after birth, especially premature infants, who have much lower antioxidant capacity than term babies [11, 12]. The switch to aerial breathing, the increased partial O_2 concentration and the stress caused by birth induces many physiological processes, most notably the neonatal adaptation to the greatly changed conditions.

Part of the adaptation is the rapid degradation of fetal hemoglobin and the oxidation of its heme moiety by heme oxygenases (HO), which are contributing factors in the development of post parturition hyperbilirubinemia. The released free heme is an aggressive oxidative agent which can be directly cytotoxic [13] and it can also become toxic by mediating oxidative stress and inflammation [14].

1.3. Oxidative stress in hemodialysed patients

The principal causes of morbidity and mortality in patients with end-stage renal disease (ESRD) requiring long-term hemodialysis (HD) are cardiovascular complications [15-17]. Even as adolescents these patients have rapidly progressing arterial diseases, arteriosclerosis, and atherosclerosis [15-17]. Previous experimental and clinical studies have highlighted the role of leukocytes in generating reactive oxygen metabolites as a primary mechanism of oxidative stress during each HD session. Additional factors include a decreased antioxidant protective capacity of uremic patients long before the initiation of maintenance HD, a status of malnutrition and/or inflammation, together with a progressive worsening of the clinical condition [17, 18]. C-reactive protein (CRP) levels are elevated in ESRD patients undergoing HD and are significantly associated with malnutrition, hypoalbuminemia, and erythropoietin resistance [17]. Asymmetric dimethylarginine (ADMA)—an endogenous inhibitor of nitric oxide synthase—levels are markedly increased in patients with ESRD as a consequence of reduced renal excretion. Both CRP and ADMA are important risk factors for cardiovascular disease and mortality in the ESRD population and are associated with increases in the incidence and progression of atherosclerotic lesions in carotid arteries. Hyperhomocysteinemia has been reported to be an independent risk factor for vascular diseases through a mechanism involving oxidative damage [19]. It has been shown that patients with ESRD have an impaired antioxidant response and therefore are at an increased

risk for inflammation, hemolysis, and arteriosclerosis [18, 20, 21]. HD treatment imposes additional oxidative stress due to the bioincompatibility of dialyzer membranes and activation of macrophages, as well as the presence of potentially toxic substances in the dialysis water supply [21].

1.4. Role of heme oxygenases

Heme oxygenases catalyze the rate-limiting step in heme degradation, resulting in the formation of iron, carbon monoxide, and biliverdin, which is subsequently converted to the antioxidant bilirubin (Bi) by biliverdin reductase [22] (Fig. 1.). Biliverdin and bilirubin are potent antioxidant themselves and play a protective role against further oxidative stress [23-26]. The transiently enhanced HO-1 mRNA accumulation is a sensitive marker of oxidative stress [27] and the induced HO-1 plays a cytoprotective role in oxidative stress and heme-mediated injury [28-30].

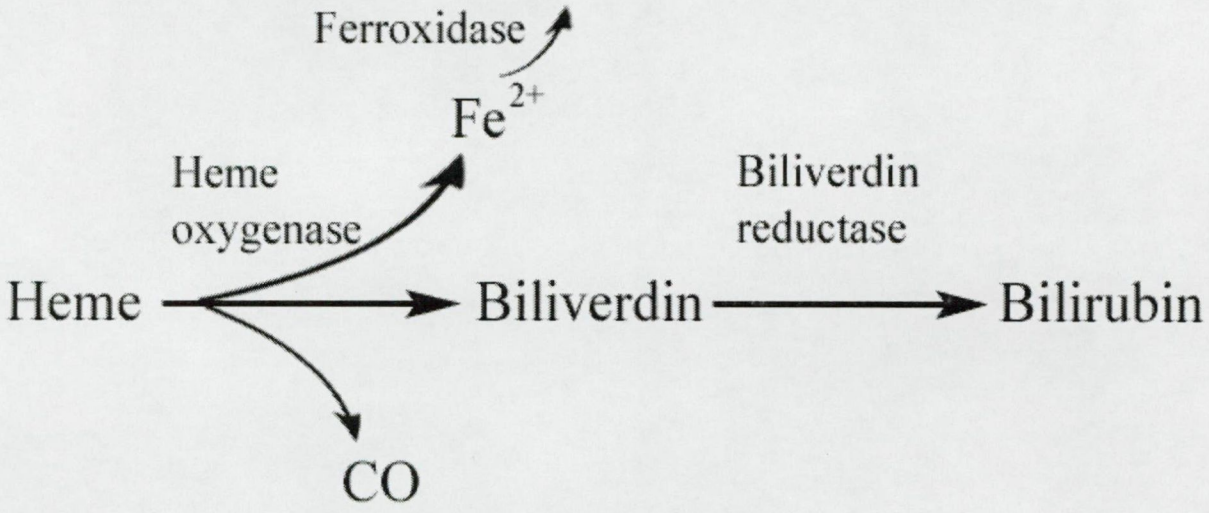

Fig. 1. The catabolic degradation of heme by Heme oxygenases.

1.4.1. Mapping

Two functional HO isoforms are known HMOX1 (GeneID: 3162, OMIM: 141250) and HMOX2 (OMIM: 141251) in humans: HMOX2 is the constitutional form, while HMOX1 is the form transcriptionally inducible by a variety of agents, such as heme, oxidants, inflammatory cytokines, UV irradiation, heavy metals and arsenite [31, 32]. Using the polymerase chain reaction for analysis of human/rodent somatic cell hybrids, Kutty et al. [33] assigned the HMOX2 gene to chromosome 16. They regionalized the assignment to 16p13.3 by FISH. Using polymerase chain reaction to study a mapping panel of human/rodent somatic cell hybrids, Kutty et al. [33] localized HMOX1 to chromosome 22. By fluorescence *in situ* hybridization (FISH), they refined the assignment to 22q12. Seroussi et al. [34] characterized a 190.3-kb contig in human 22q13.1 and identified the HMG2L1 (High Mobility Group Protein 2-Like 1) and TOM1 (Target of MYB1) genes, as well as the previously identified HMOX1 and MCM5 (Mini Chromosome Maintenance homolog 5) genes. The order of these genes is cen--HMG2L1--TOM1--HMOX1--MCM5--tel. All are oriented in a 5-prime to 3-prime direction from centromere to telomere.

1.4.2. Animal model

Growth retardation, anemia, iron deposition, and vulnerability to stressful injury are all characteristics observed in mice in whom the heme oxygenase-1 gene has been knocked out [35]. Wagener et al. [36] investigated the involvement of heme and its degrading enzyme heme oxygenase in the inflammatory process during wound healing, studying Wistar rats. They observed that heme directly accumulates at the edges of a wound and that this coincided with an increased adhesion molecule expression and the recruitment of leukocytes. Intradermal administration of heme 24 hours before injury resulted in heme-induced influx of both macrophages and granulocytes. Heme-oxygenase 1 was significantly expressed in the epithelium of both the mucosa and the skin of animals without wounds. On inflammation, its expression increased, particularly in infiltrating cells during the resolution phase of inflammation. They interpreted their results as indicating that local release of heme may be a physiologic trigger to start inflammatory processes, whereas heme oxygenase 1 antagonizes inflammation by attenuating adhesive interactions and cellular infiltration. The basal level of heme oxygenase expression in the skin may serve as a first protective environment against acute oxidative and inflammatory insults.

1.4.3. Clinical features

Yachie et al. [37] reported the first human case of heme oxygenase-1 deficiency. Sequence analysis of the patient's HMOX1 gene showed complete loss of exon 2 of the maternal allele and a 2-nucleotide deletion in exon 3 of the paternal allele; a normal HMOX1 gene contains 5 exons. The patient was 26 months old when he was first brought for medical care because of recurrent fever and generalized erythematous rash. Growth retardation was apparent and marked hepatomegaly was noted, but the spleen was not palpable. Asplenia was confirmed by abdominal ultrasonography and isotope image scanning. Hematuria and proteinuria were consistently present. At 6 years of age, the boy had severe growth retardation. Persistent hemolytic anemia was characterized by marked erythrocyte fragmentation and intravascular hemolysis, with paradoxical increase of serum haptoglobin and low bilirubin. They described severe persistent endothelial damage at the patient. Electron microscopy of renal glomeruli revealed detachment of endothelium, with subendothelial deposition of an unidentified material. Iron deposition was noted in renal and hepatic tissue. Immunohistochemistry of hepatic tissue and immunoblotting of a lymphoblastoid cell line revealed complete absence of heme oxygenase-1 production. A lymphoblastoid cell line derived from the patient was extremely sensitive to hemin-induced cell injury.

1.4.4. Role of HOs during oxidative stress

Much controversy exists regarding the predominant effect of HOs in the setting of oxidative injury (Fig 2.). This is rooted in the further biochemistry of heme breakdown products [38]. HOs may have a pro-oxidant effect, as the iron released from heme (in the setting of low ferritin availability) may react with hydrogen peroxide via the Fenton reaction to form hydroxyl radicals [39-41]. On the other hand producing biliverdin and its metabolite bilirubin, however, HOs may act with an antioxidant effect [42, 43], because bilirubin is a potent antioxidant [23-26]. The effect of HOs on oxidative cell injury may vary considerably with cell type, level of expression, and chemical properties of the oxidant [39, 44-46]. Furthermore, HOs convert a lipid-soluble oxidant (heme) into iron, which can be sequestered with ferritin, when available. This protects the cell from lipid peroxidation that would otherwise occur, particularly considering the affinity of heme for the hydrophobic cell membrane interior [47].

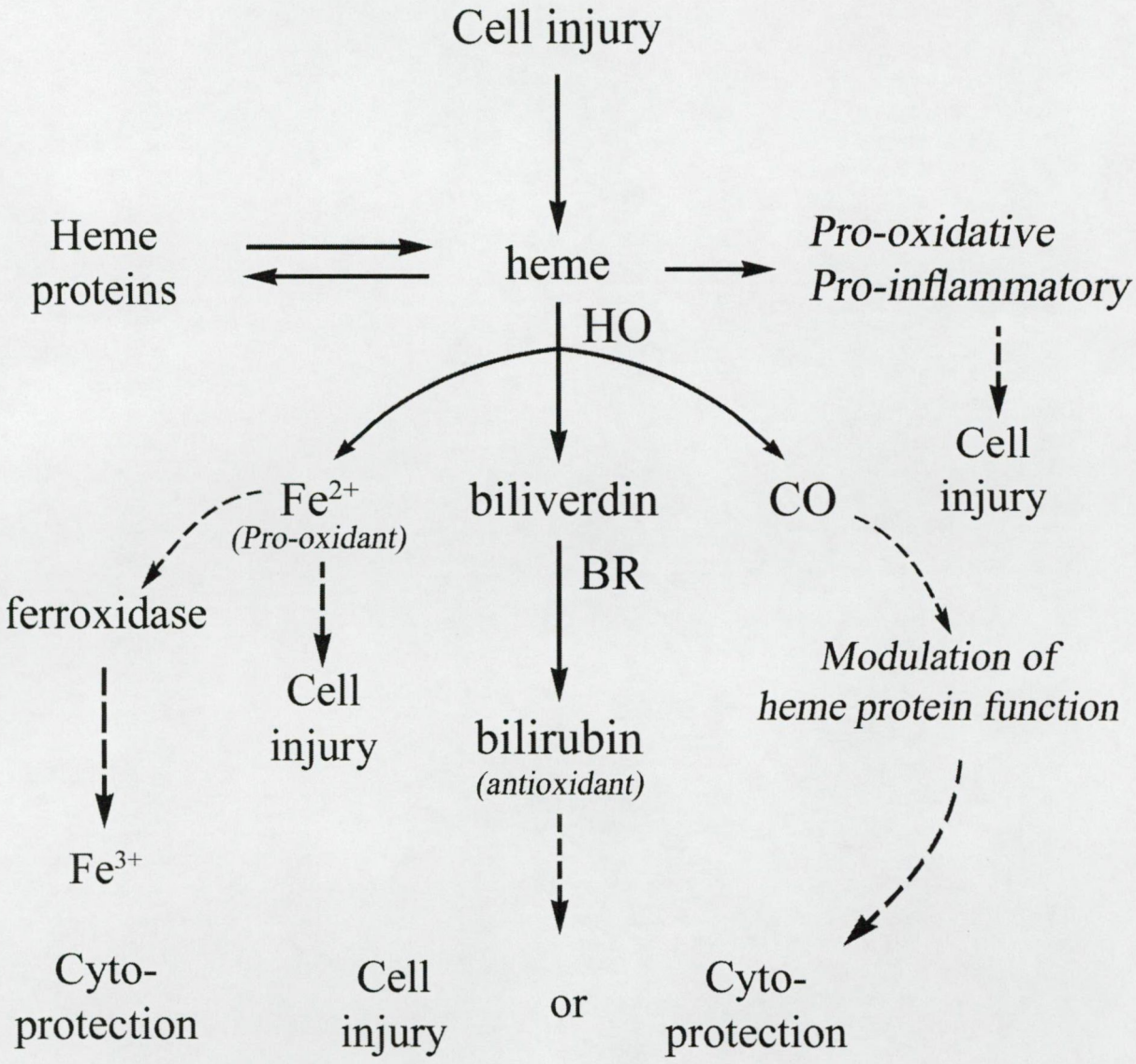

Fig. 2. The breakdown of heme. Heme derived from hemoglobin in senescent erythrocytes, other heme proteins, or newly synthesized is degraded by HO into biliverdin, CO, and iron. Biliverdin gets converted into the anti-oxidant bilirubin by biliverdin reductase. Ferric iron (Fe^{3+}) is directly sequestered by ferritin. CO can interact with heme proteins (e.g., guanylyl cyclase) and alter their activity. Heme and its breakdown products possess various physiological properties but are also potentially toxic.

1.3. The aim of the study

1. To date, the genetic basis of Costello syndrome is unknown therefore our aim was to refine the break point regions of a Costello syndrome patient with an apparently balanced chromosomal translocation t(1;22) (q25;q11) at the molecular level by FISH.

2. There was a need to establish a scaleable and sensitive method to measure the HO-1 expression because of the limited amount of samples available from premature.

3. Although HO-1 induction may be a general and adaptive response to oxidant stress, the inducibility of this enzyme in the early postnatal period in human newborns had not been studied yet. We hypothesized that enzymatic immaturity of HO-1 or its regulation system could play a role in the early transitory adaptation disturbances of premature neonates. Therefore our aim was to investigate the HO-1 expression in mature and premature neonates during the fist week after birth to find out if the enzyme is inducible and whether there are any differences between the two groups.

4. The changes in Hb metabolism in uremic patients are the major cause of HD-mediated endothelial injury. Therefore our aim was to follow the effects of single HD sessions on the plasma hemoglobin and bilirubin as indicators of hemolysis, the ferroxidase activity, the erythrocyte-derived reduced and oxidized glutathione levels and HO-1 mRNA expression as oxidative stress markers, and the homocysteine levels as and independent risk factor.

2. METHODS AND PATIENTS

2.1. Methods used in the positional cloning experiments

2.1.1. Cultivation of Yeast artificial chromosome (YAC), P1-artificial chromosome (PAC), Bacterial artificial chromosome (BAC) and cosmid clones

The selected yeast strains containing our YAC inserts were spread and incubated on plate for 2-3 days on 30°C on DOB medium with CSM -TRP -URA (0.7 gr/l) according to Burke et al. [48]. Single colonies were innoculated in 2ml of DOBA (43.7 gr/l) medium and incubated for 1 day on 30°C on a shaker. The yeast strains were transferred in 50ml DOBA medium (43.7 gr/l) and incubted for 2 days 30°C on a shaker. PAC, BAC, and cosmid cultures were grown in 2ml of LB medium in the presence of the appropriate antibiotic at 30°C until an OD600 of 0.6 0.8 was reached.

2.1.2. Isolation of the DNA insert from YAC, PAC, BAC and cosmid clones

The protocol to separate yeast DNA from the culture was based on that of Philippsen et al. [49]. The obtained yeast chromosomes were run on a 1.2% low-melting-point agarose gel by pulse field electrophoresis (initial time 70 s, final time 90 s, 6 V/cm, for 24 h). Gels were stained for 15 minutes with ethidium bromide and subjected to UV light for visualization of the DNA. The extra bands containing the YAC insert were cut out by scalpel. The DNA was isolated from the low-melting-point agarose and purified. For PAC, BAC and cosmid clones DNA was prepared from 2 ml of culture using a standard alkali miniprep protocol [50].

2.1.3. Fluorescence *in situ* hybridization (FISH) experiments

The chromosomes and nuclei spread was prepared from metaphase stopped fibroblast culture of the patient as described in Kutsche et al. [51]. The probes were nick translated with biotin-dUTP (Nick Translation System, Gibco BRL, Gaithersburg, MD). The YAC, PAC, BAC, cosmid probes were labeled by fluorescein isothiocyanate (FITC). Additionally a TEL 1q DNA probe labeled with Texas red was used to visualize chromosome 1. The

chromosomes were counterstained with 4',6-Diamidino-2-phenylindole (DAPI).

2.2. Methods used in the gene expression experiments

2.2.1. RNA extraction and competitive reverse transcriptase (cRT)-PCR experiments

The Human DNA sequence from clone CTA-286B10 on chromosome 22 (Nucleotide accession no: Z82244, GenBank: 3191962) was used to design the primers for the experiments. The primers were designed by the *OLIGO* software package. Since the clone contained the genomic sequence of HMOX1 thus we could design the primers to span exon boundaries to avoid binding of primers at DNA level (Fig. 3A). The amplicon and primer binding sites were checked by RepeatMasker and BLAST-ed to database 'nr' to avoid designing primers into repeat regions or other conservative protein motifs.

The mRNA was extracted from 1 ml (100µl in case of neonates) of venous blood with the mRNA Isolation Kit for Blood/Bone Marrow (Roche Diagnostics, Mannheim, Germany). Competitive reverse transcriptase PCR was used to identify the expression of heme oxygenase-1 gene. The competitor RNA was created by in vitro mutagenesis from HMOX1 cDNA and transcription with T3 RNA polymerase (Fermentas AB, Vilnius, Lithuania) according to Waha et al. [52]. The primers to generate the competitor were as follows:

HMOX1-T3 5′ AAT TAA CCC TCA CTA AAG GGA GAC GTT TCT GCT CAA CAT CCA GCT C 3′

HMOX1-mut 5′ CCT GGG AGC GGG TGT TGA GTG GGG GGC AGA ATC TTG CAC TTT G 3′

To avoid error due to RNA degradation the competitor RNA fragment was diluted and aliquoted into *Eppendorf* tubes (3 µl / tube) and stored on minus 70°C till usage. For each measurement a new tube of competitor RNA was thawed and used with freshly separated HMOX1 mRNA for the RT step.

First-strand cDNA was generated by using the RevertAid First Strand cDNA Synthesis Kit (Fermentas AB) with the specific primer of HMOX1-R. To avoid pipetting

errors the method described in the cDNA synthesis protocol was altered (Table 1.). We dissolved HMOX1 mRNA in 5 times more RNase free water and we used an extra 6 times dilution step at the preparation of competitor RNA dilutions.

Table 1. Altered cDNA synthesis mix

	original protocol	**altered protocol**
HMOX1 mRNA	1 µl	**5 µl (5x diluted)**
Competitor mRNA	1 µl	**6 µl (6x diluted)**
100 nM HMOX1-R	1 µl	**1 µl**
RNase free H_2O	9 µl	-
10 mM dNTPs	2 µl	**2 µl**
RNase inhibitor	1 µl	**1 µl**
5x synthesis buffer	4 µl	**4 µl**
reverse transcriptase	1 µl	**1 µl**

For practical reasons (amount of sample available, expected range of HMOX1 mRNA induction) we used a four step (3x) dilution of competitor RNA.

The PCR amplification was carried out with the following program: initial denaturation at 94°C for 5 min, followed by 25 cycles of denaturation at 94°C for 20 s, annealing at 61°C for 30 s and extension at 72°C for 20 s, followed by a final extension at 72°C for 10 min. The primers were as follows:

HMOX1-F 5′ CGT TTC TGC TCA ACA TCC AGC TC 3′

HMOX1-R 5′ CCT GGG AGC GGG TGT TGA GTG 3′

The amplified cDNAs were examined on 6% polyacrylamide gels and stained with ethidium bromide. The target HMOX1 band was calculated by the ratio to the competitor by densitometry (AlphaImager, AlphaEase 5.5) (Fig. 3B). HMOX1 mRNA concentrations were expressed with reference to the white blood cell count; since we did not calculate the copy number of our control RNA, these are relative values (we used the same dilutions of control RNA). Control RNA and mRNA were handled together in the same tubes, their relative ratio

therefore remaining the same throughout the whole process.

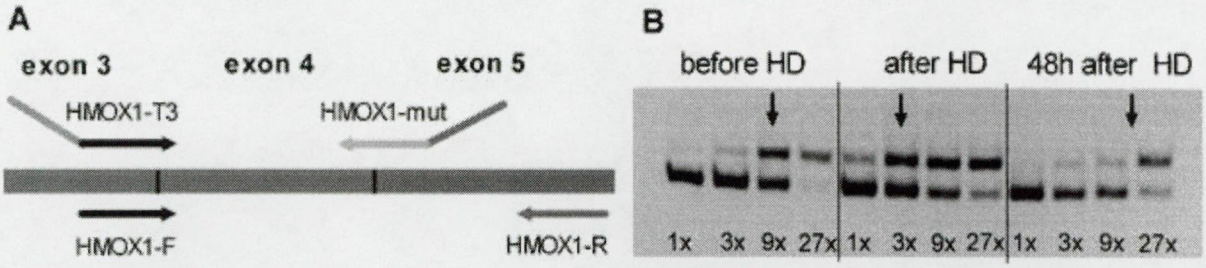

Fig. 3A. Part of HMOX1 CDS from exon 3 to 5, HMOX1-T3 and HMOX1-mut were used to create a polymerase chain reaction (PCR) product from which we transcribed our control RNA, the sequence of which differs from that of wild-type HMOX1 mRNA in only a 20-bp deletion. The mRNA and control RNA were reverse transcribed and consecutively amplified by the same primers HMOX1-F and HMOX1-R.
B HMOX1 mRNA expression of a patient with oxidative hemolysis before, after and 48 h following hemodialysis (HD). A four-step (3x) dilution of control RNA was reverse transcribed with equal amounts of mRNA and amplified by the same PCR primers. The *arrows* show where the mRNA concentration is equal to the control RNA concentration

2.2.2. Biochemical methods

Blood Hb concentration was measured with an OSM 3 Hemoximeter (Radiometer, Copenhagen, Denmark). For the assay of plasma Hb and its oxidized metabolites, metHb and hemichrome, heparinized plasma samples were diluted 1:40 (v/v) with 5 mmol/L PBS, pH 7.4, and measured spectrophotometrically at different wavelengths according to the method of Winterbourn [18]. Plasma concentrations of the unbound Bi were estimated by spectrophotmetric method of Jacobsen and Wennberg [53]. The total ferroxidase (FOX) activity and the ceruloplasmin ferroxidase activity in the plasma were measured with conalbumin according to Johnson et al. [54]. Homocysteine concentrations were measured by HPLC according to Feussner et al. [55].

Reduced (GSH) and oxidized glutathione (GSSG) concentrations were measured separately in the whole blood by a combination of previously accepted standard methods [56], and were expressed with reference to Hb determined by the cyanmethemoglobin method.

All biochemical measurements were performed in duplicate. The precision of the methods was followed by estimating the coefficients of variation (CV). The intra- and interassay CVs for all the biochemical analyses were between 3.0 and 6.0%.

2.3. Patients

We analyzed the Costello syndrome patient (a Hungarian girl) described by Czeizel and Timar [10]. We had fibroblast cells which were cultured and used for the FISH experiments.

We analyzed the HO-1 mRNA expression in three groups of patients. The mature neonate patient group was obtained from the Department of Gynecology, the premature neonate group was obtained from the perinatal intensive center of Department of Pediatrics. The young adult hemodialysed patients were obtained from the hemodialysis center of the Department of Pediatric.

2.3.1. Characterization of the Costello syndrome patient

The Hungarian girl with Costello syndrome had an apparently balanced translocation: 46,XX t(1;22)(q25;q11). The karyogram of the patient is shown on Fig. 4. The patient showed excessive generalized skin, more pronounced in the palms, 'wash woman's hands,' and soles, with elastolysis confirmed by histologic examination. The long tubular bones were osteoporotic. Spina bifida occulta was demonstrated in L5 and S1. Mental retardation was mild. She had a particularly sociable and humorous personality.

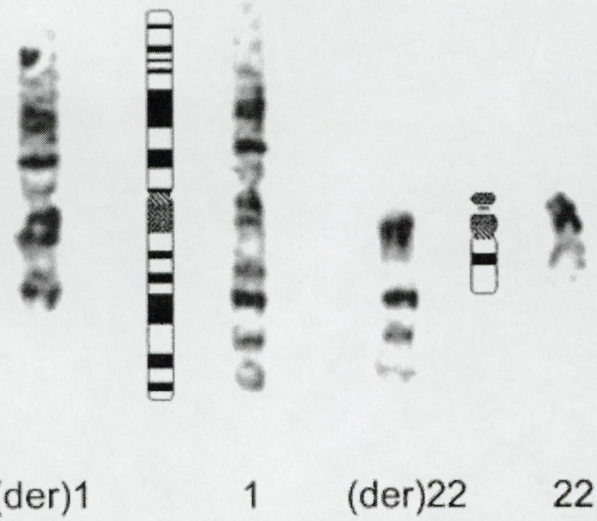

Fig. 4. Chromosome 1;22 translocation in the patient. GTG-banded pairs of the patient with an apparently balanced and reciprocal translocation [t(1;22) (q25;q12)] are shown and ideograms of wild-type chromosomes 1 and 22.

2.3.2. Characteristic of mature and premature neonates

We analyzed 21 mature (gestational time are 37-40 weeks, birth weight: median 3305g; quartiles 3060g, 3770g) and 20 premature neonates (gestational time are 26-36 weeks, birth weight: median 1860g; quartiles 1450g, 2230g) with transient neonatal adaptation difficulties. We excluded babies with respiratory distress, sepsis, positive bacteriology or any serious complication (intracerebral hemorrhage, necrotizing enterocolitis, pneumonia, pneumothorax, and any congenital heart disease). None of the examined patients were on mechanical ventilation (>24h) and none of them had blood transfusion during the investigation period.

The indication of phototeraphy was according to the practice written in "Care of the High-Risk Neonate" [57]. The patients requiring phototherapy were on intermittent therapy (425-475 nm light/normal light in 4 hour intervals). None of the mature neonates had to be supplied with extra O_2. Ten premature neonates with a transitory adaptational disturbance were on extra O_2 (<24 h). Indication of extra oxygen support was determined by PaO_2 values (the PaO_2 levels were kept in the range of 50-70 mmHg in term newborns, and 40-60 mmHg in prematures with less than 1500 g birth weight). The FiO_2 values in these patients were 0.4 (quartiles 0.3, 0.6).

Whole blood samples were collected in EDTA microtainer tubes (approx. 200 µl per sample) during the first week following birth. For mRNA analysis 100µl were pipetted out immediately into 1ml RNA stabilization reagent. Quantitative blood count was performed on an ABX Micros 60 hematological automat.

We obtained blood samples from mature newborns in parallel with the routine serum bilirubin assay, usually 2-3 samples from each babies before they left the obstetrical ward. We obtained blood samples from premature newborns each day following birth (7 samples from each babies).

2.3.3. Characteristic of HD patients

17 HD patients dialyzed in our dialysis unit were included in the study. The duration of HD treatment in these 17 patients was 38 months (median, quartiles: 16; 102). The patients were grouped according to the duration spent in the dialysis program: short-term HD patients (n=7, median 19 months, quartiles: 9, 29) and long-term HD patients (n=10, median 97 months, quartiles: 53, 150). Age, sex, weight and height distribution of the two groups are displayed in Table 2. As controls for the biochemical data, age- and sex-matched healthy young adult patients were selected from among subjects before undergoing orthopedic surgery (n=20).

Table 2. Demographic characteristics of uremic patients on HD (means ± SD)

	Short-term HD (n=7)	Long-term HD (n=10)
Demographic characteristic of patients		
Age (y)	27.8 ± 4.8	25.1 ± 4.4
Sex (M/F)	4/3	5/5
Weight (kg)	53.7 ± 16.2	58.1 ± 18.1
Height (cm)	159.6 ± 15.2	164.71 ± 37.1

The distribution of the original nephrological diagnosis in the ESRD group was as follows: chronic pyelonephritis with reflux nephropathy 7, interstitial nephritis 3, membranoproliferative glomerulonephritis 4, focal segmental glomerulosclerosis 2, and rapidly progressive glomerulonephritis 1. All these patients had been on antihypertensive therapy with a combination of angiotensin-converting enzyme inhibitor and calcium channel blocker, and had received 4-h bicarbonate HD 3 times a week with a hemophan single-use dialyzer. The blood flow rate was 200 ml/min and the dialyzate flow rate was 500 ml/min. During HD, Na-heparin was used as an anticoagulant, in an initial dose of 500 IU, followed by continuous infusion at a rate of 1000 IU/h. Erythropoietin treatment was started depending on hematocrit and hemoglobin status of uremic patients even before the entry to the HD

program. Erythropoietin was given in the range of 30-70 IU/kg/dose post HD after the collection of blood samples. We used the formula Kt/V for the evaluation of dialysis efficiency; the target value was >1.1.

Blood samples were collected before, immediately after and 48 h following HD. For the analysis of biochemical parameters, 1 ml of anticoagulated (with EDTA and heparin) blood was collected. For mRNA separation 1 ml of native blood was collected and stabilized in RNA/DNA Stabilization Reagent for Blood/Bone Marrow (Roche Diagnostics GmbH, Germany).

2.4. Statistical analysis

Clinical data on the patients are reported as means ± standard deviations (x ± SD), while results of biochemical analyses are shown in figures as means ± standard errors (x ± SEM). Statistical analyses included both parametric (variance analysis, Tukey test and Student's t-test, unpaired t-test) and non-parametric tests (Wilcoxon rank test). When the extent of variance between pairs of groups differed significantly from each other ($p < 0.05$ in the F-test), we used the Welch test (d probe) instead of the t test to compare the mean values. Correlations between parameters were characterized by calculation of the linear regression and correlation coefficients. The level of significance for all tests was taken as 0.05.

3. RESULTS

3.1. FISH analysis of the break point regions of the Costello syndrome patient

We have re-analyzed the chromosomes of this translocation patient by high-resolution banding (450- to 550-band level) that confirmed the breakpoint on chromosome 1q25, and refined that on chromosome 22 to q12 (Fig. 4.). In order to delineate and define the breakpoint regions at the molecular level, FISH analysis was done by YAC, PAC, BAC, and cosmid clones from the corresponding chromosomal regions (for methodological details, see Kutsche et al. [2000]). For the chromosome 1q25 breakpoint, the YAC clone, 786G11 (530 kb), positive for microsatellite marker D1S2659, was found to hybridize proximal to the breakpoint, whereas two YACs, 807D10 (1,790 kb), positive for marker D1S2640, and clone 949G05 (1,260 kb), positive for marker D1S222, hybridized distal to the breakpoint (data not shown). Based on this data, we selected YAC clone 790F06 (1,390 kb), positive for microsatellite marker D1S3424 that, indeed, hybridized to both rearranged chromosomes 1 and 22 (and to wild-type chromosome 1), confirming the position of the breakpoint in 1q25 (data not shown). For further analysis, three additional YACs from the putative breakpoint region were tested by FISH. YAC clone 745G01 (570 kb), positive for D1S3424 and SOAT1, hybridized distal to the breakpoint, whereas YACs 897A04 (650 kb), positive for D1S2425 and D1S2078, and 896A03 (1,130 kb), positive only for D1S2425, hybridized proximal to the breakpoint (Fig. 5A). Thus, it seems that YAC 790F06 spans the breakpoint on chromosome 1q25 mapping it between markers D1S2078 and SOAT1 (Fig. 5A). Subsequently, 43 PAC clones were isolated and 14 placed in order to form a partial contig using microsatellite and end-sequence STS markers derived from selected PAC clones (Fig. 5B). Of the ramdomly selected PACs analyzed in FISH experiments, 10 clones hybridized proximal, and three clones distal to the 1q25 breakpoint, whereas PAC K1443 was spanning it (Fig. 6, data not shown). BlastN analysis of end-sequences generated from K1443 has revealed that one end corresponds to position 1628097 in the genomic sequence of contig NT_026949 and the other one to position 1747898, giving an insert of 109801 bp. BLAST searches with this 109 kb sequence revealed homology to three different EST clusters (UniGene data set Hs.102398, Hs.74104, and Hs.5415) suggesting that at least one gene is located on the breakpoint spanning PAC clone on chromosome 1.

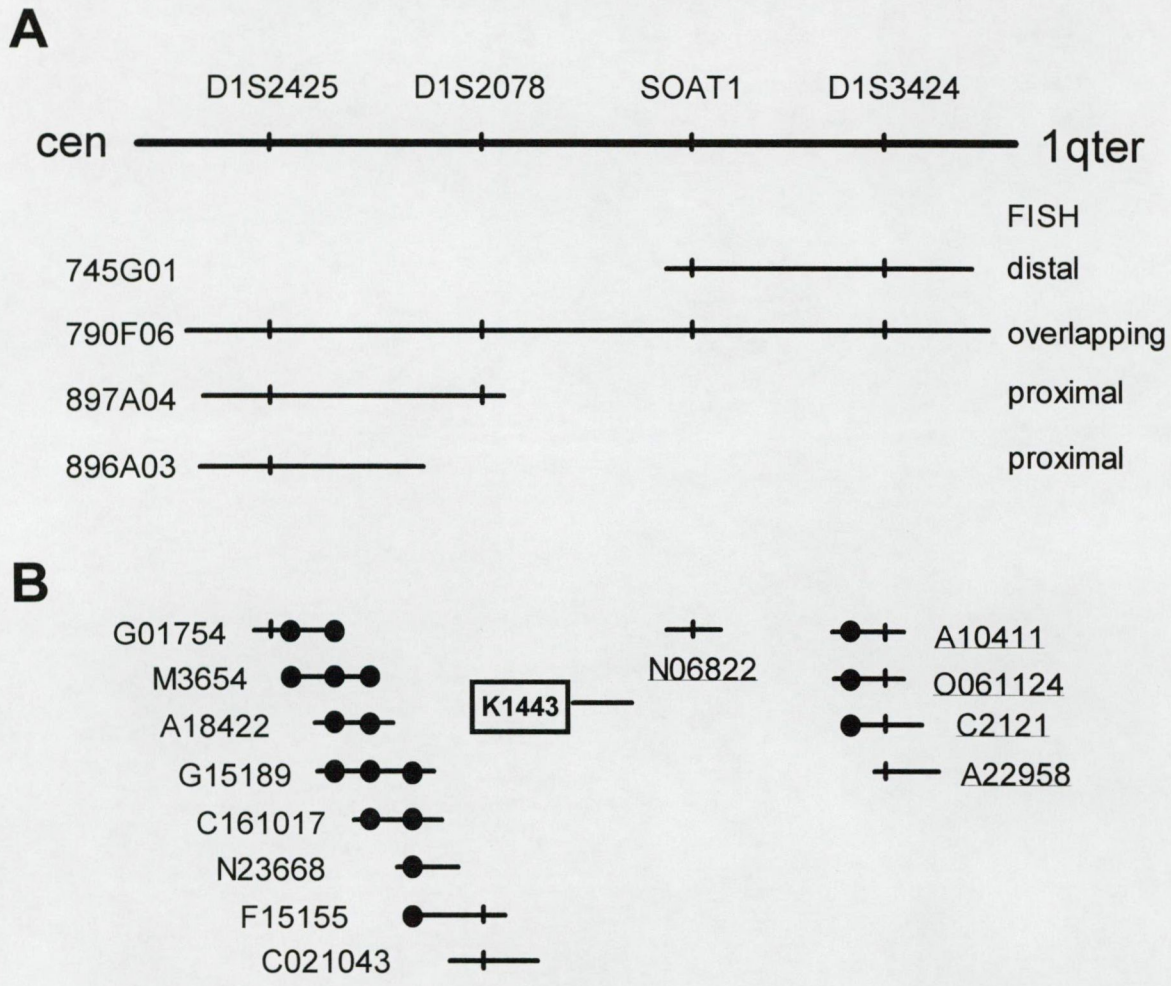

Fig. 5. Characterization of the translocation breakpoint in 1q25. **A:** Delineated breakpoint region and position of four YACs on chromosome 1q25. The upper line represents a region from 1q25 from centromere to telomere that is not drawn to scale. Microsatellite markers are indicated by vertical bars. YAC inserts are shown by black lines. Data of FISH analysis with each of the YAC clones are indicated on the right. **B:** Partial PAC contig in 1q25. PAC clones are represented by black lines. Microsatellite markers are indicated by vertical bars, and STS end-markers by filled circles. PAC clone K1443 (framed) is spanning the breakpoint in FISH experiments. PAC clone mapping proximal to the breakpoint are on the left, whereas those located distal to the breakpoint are grouped on the right.

The breakpoint on chromosome 22 was originally localized by conventional cytogenetic analysis and assigned to q11 [10]. Since reinvestigation by high-resolution banding suggested that the breakpoint was in q12 (Fig. 4), we performed FISH experiments by YAC clones from 22q11-q12.

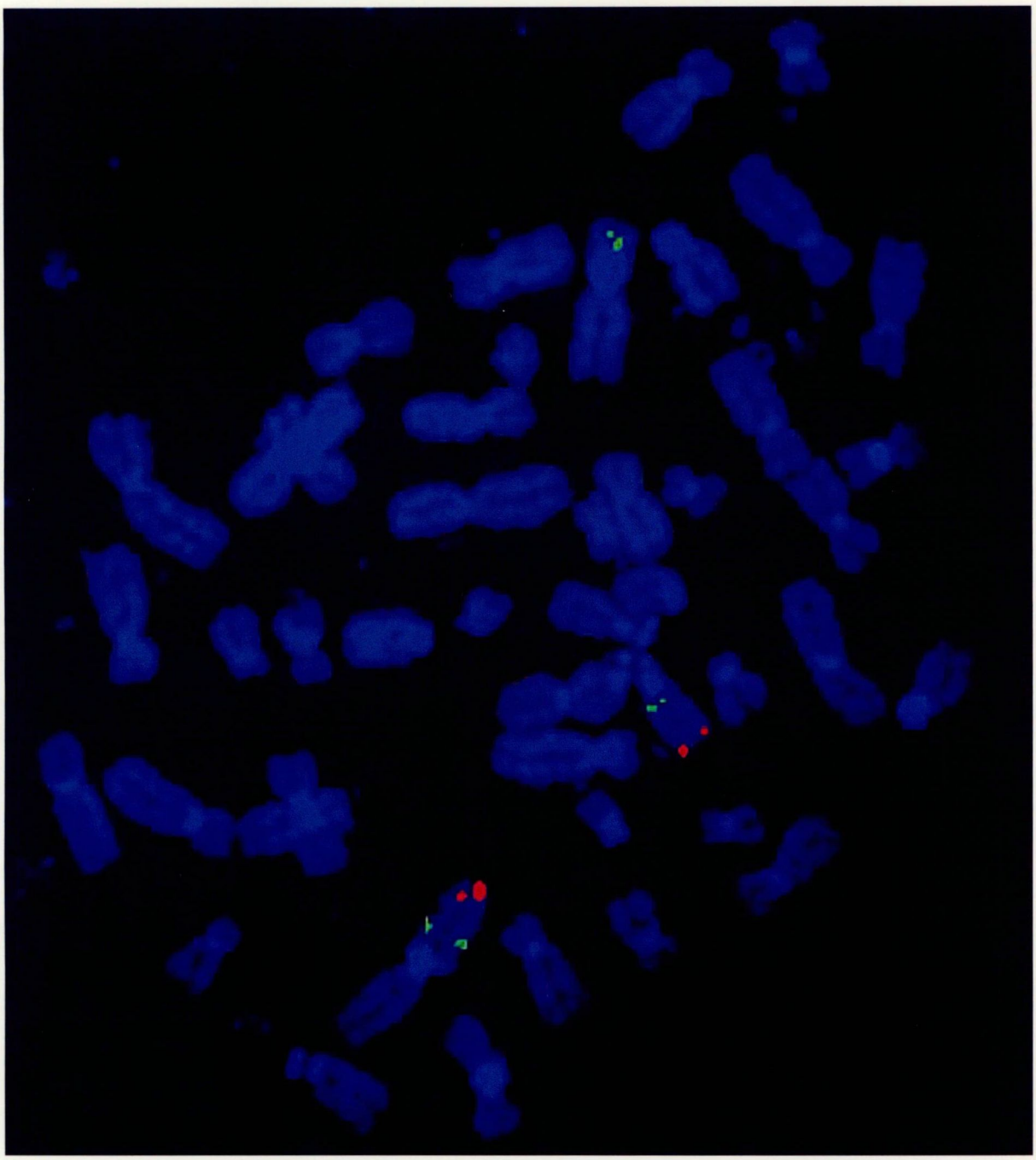

FIG 6. FISH with PAC clone K1443 hybridized to lymphocyte metaphase spreads of the patient. The probe is labeled by FITC (green). PAC K1443 produces a signal on the wild-type chromosome 1 (q25), as well as on der(1) and der(22), indicating that this clone is spanning the breakpoint. A TEL 1q DNA probe labeled by Texas red (red) was used to identify the telomere of the long arm of chromosome 1. Chromosomes are counterstained with DAPI.

Three YACs, 848D02, 891F12, and 742B05, hybridized on several chromosomes, indicating that these clones were chimeric (data not shown). Two clones, 765E02 (500 kb), and 881H10 (650 kb) hybridized proximal to the breakpoint (Fig. 7A) suggesting that the breakpoint region is more telomeric. Similarly, seven additional YAC clones, cytogenetically assigned to 22q11.2 to q13.1, hybridized proximal to the breakpoint (Fig. 7A). In contrast, two YACs, 803D03 and 924C02, mapped to the end of 22q13.1 and the beginning of q13.2, hybridized distal to the breakpoint (Fig. 7A).

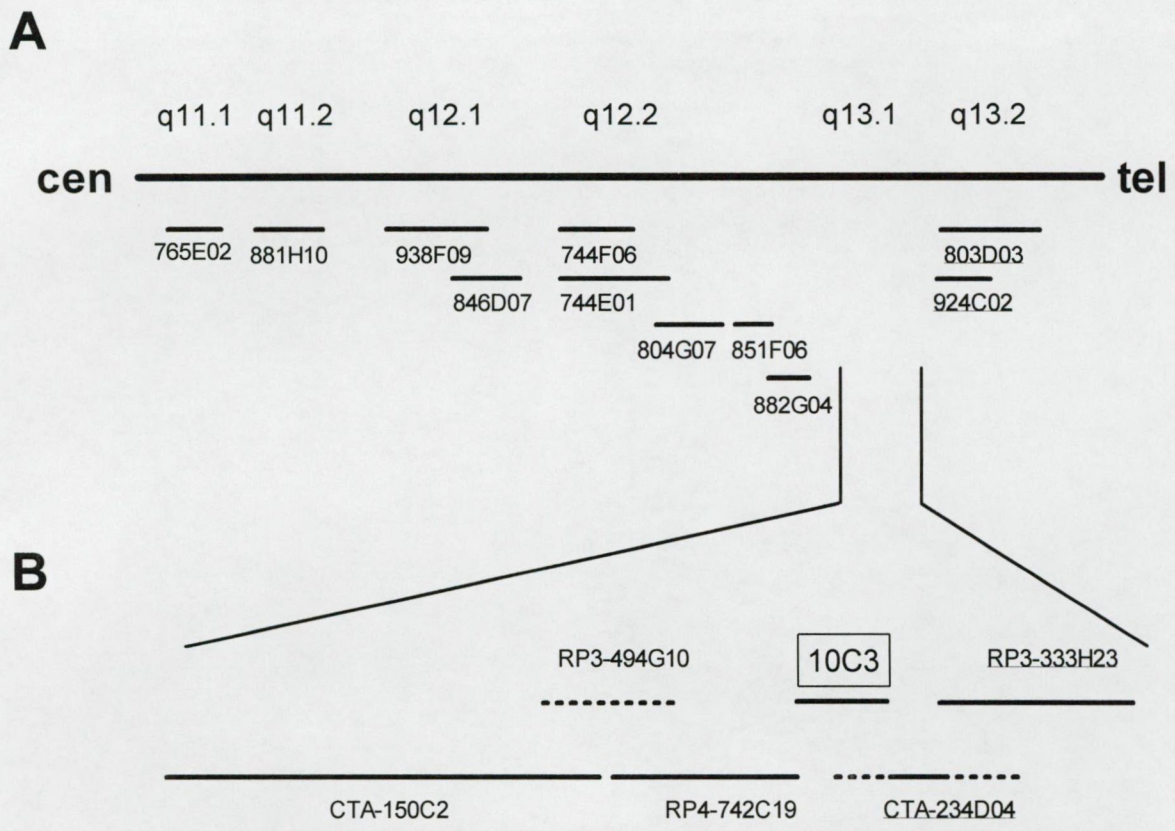

Fig. 7. Characterization of the translocation breakpoint in 22q11-q13. **A:** The upper line represents a region of 22q11 to q13.2 in centromere to telomere orientation that is not drawn to scale. YAC inserts are shown by black lines. YAC clones hybridizing proximal to the breakpoint are on the left, whereas those hybridizing distal to the breakpoint (underlined) are grouped on the right. **B:** In the insert, BAC, PAC, and cosmid clones analyzed in FISH experiments are shown. Black lines represent sequenced regions of these clones. The three PAC/BAC clones on the left hybridized proximal, the two on the right (underlined) distal to the breakpoint, whereas cosmid LL22NC03-10C3 (framed) spanned it.

Fig 8. FISH with cosmid clone 10C3 hybridized to lymphocyte metaphase spreads of the patient. The probe is labeled by FITC (green). Cosmid 10C3 produces a signal on the wild-type chromosome 22 (q13), as well as on der(1) and der(22), indicating that this clone is spanning the breakpoint. A TEL 1q DNA probe labeled by Texas red (red) was used to identifiy the end of the long arm of chromosome 1. Chromosomes are counterstained with DAPI.

Based on this data, FISH analysis refined the cytogenetic breakpoint from 22q11 to 22q13.1. No YAC clone was found located in the putative breakpoint region. Instead, numerous PAC, BAC, and cosmid clones have been used for further FISH experiments. Of these, three PAC/BAC clones, CTA-150C02, RP3-494G10, and RP4- 742C19, hybridized

proximal and two, CTA-234D04 and RP3-333H23, distal to the breakpoint, whereas cosmid LL22NC03-10C3 spanned the breakpoint (Fig. 7B, Fig. 8, data not shown). Analysis of the DNA sequence of chromosome 22 deposited in the database (NT_011520) revealed that the gene encoding the platelet-derived growth factor beta (PDGFB) is located on the insert of the cosmid.

3.2. Established a sensitive cRT-PCR method

For the synthesis of the competitor fragment we separated mRNA from the blood of a healthy person. This mRNA was reverse transcribed by the specific HMOX1-R primer and amplified by PCR with the primers HMOX1-F and HMOX1-R. The size of product was verified by gel electrophoresis. This cDNA fragment was then used for PCR based the *in vitro* mutagenesis to create a 20 base pair internal deletion and to add a T3 RNA polymerase binding site. We verified the cDNA fragment we used to transcribe the competitive RNA fragment with restriction enzyme digestion (Ava II). By electrophoresis we proved that we got a specific product from HO-1 mRNA which contains the 20 base pair deletion (Fig. 9). The measured sizes of products were in correspondence with the expected undigested and digested sizes.

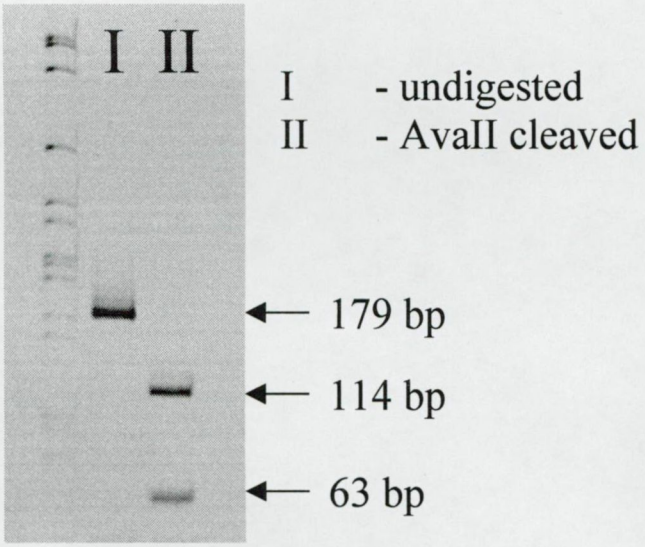

Fig 9. AvaII digestion of cDNA fragment used to transcribe the competitor RNA. The DNA was run on 8% polyacrylamide gel, and stained with ethidium bromide. Fragment sizes were analysed by AlphaImager AlphaEase 5.5

Furthermore we also confirmed that HMOX1-F and HMOX1-R primer pair which were designed on exon boundaries does not amplifies unspecific products. We got no unspecific

amplicon when genomic DNA was used as template and proved that our primers bound only to cDNA reverse transcribed from HMOX1 mRNA. The expression range of HO-1 in neonates and uremic patients and the corresponding competitor RNA fragment dilutions were determined by analyzing 3-3 samples in a pilot study before our experiments.

3.3. HO-1 expression in mature and premature neonates

The hemoglobin (Hb), mean corpuscular volume (MCV), WBC, and platelet count (PLT) for the mature and premature newborns were in the normal ranges (Table 3) and their changes during the first week excluded the presence of severe anemia, sepsis or inflammation.

Table 3. Blood count parameters of mature and premature neonates (x ± SD)

	Mature neonates n = 21			**Premature neonates n = 20**		
	day 1	day 3	day 5	day 1	day 3	day 5
Hb (g/l)	159.6±19.6	155.4±23.1	156.6±29.8	184.8±16.0***	187.0±18.5***	172.7±18.8***
MCV (fl)	110.7±2.9	110.1±4.7	108.4±4.5	109.1±3.8	108.2±3.6	106.2±4.3
PLT (10^9/l)	187.5±84.1	198.7±79.3	243.1±112.6	233.3±67.4***	248.7±56.7***	280.2±96.6***
WBC (10^9/l)	14.75±4.80	9.91±4.01	10.1±4.30	19.3±2.56**	10.83±1.77	10.10±2.23

t test: *** P<0.001; ** P<0.005 healthy premature vs. mature neonates

The relative HO-1 mRNA levels of the mature and premature neonates are shown in Fig. 10. The levels and inducibility of HO-1 in the two groups proved similar. HO-1 expression was induced on days 2 and 3. Later, the HO-1 mRNA levels decreased and dropped below the day 1 value by the end of the first week.

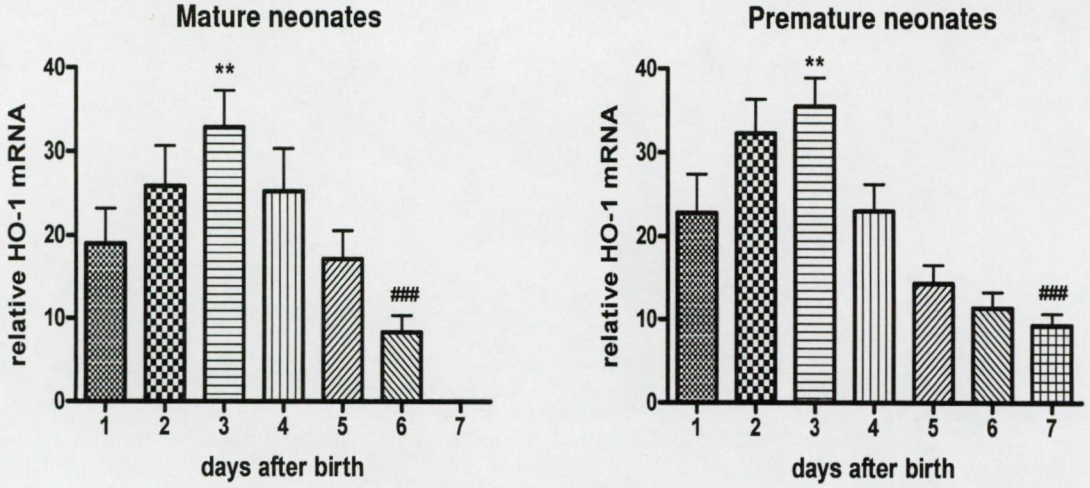

Fig. 10. Relative HO-1 mRNA levels during the first week after birth in healthy mature and premature neonates. Unpaired *t* test: ** P<0.005 day 3 *vs.* day 1; ### P<0.001 last day sample *vs.* day 3.

The serum bilirubin levels of the mature and premature neonates are shown in Fig. 11. These levels increased significantly after birth in both groups, and were the highest on day 5 after birth.

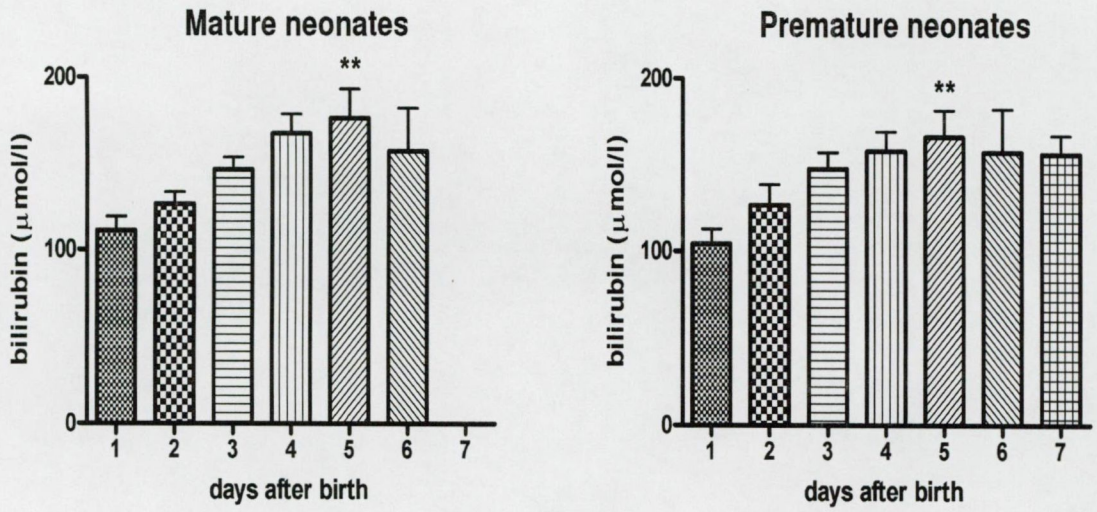

Fig. 11. Bilirubin levels during the first week after birth in healthy mature and premature neonates. Unpaired t test: ** P<0.005 day 5 vs. day 1.

3.4. HO-1 expression in young hemodialysed uremic patients

Blood and serum values of controls and hemodialysed patients are displayed in Table 4. Both the GSSG concentration and the glutathione redox ratio (GSSG/GSH) were significantly higher in the HD patients than in the controls (Table 4). The FOX activity in the HD patients (0.89±0.03 before HD) was significantly ($P<0.01$) higher than that in the controls (0.59±0.01) (Table 4).

Table 4. Concentrations of some biochemical parameters in the whole blood and in the plasma of the study population (means ± SEM)

	Controls (n=20)	HD patients (n=17)		
		before HD	Immediately after HD	48 h after HD
Whole blood values				
Reduced glutathione (GSH) (μmol/g Hb)	7.36 ± 0.20	7.46 ± 0.28	7.69 ± 0.28	7.72 ± 0.30
Oxidized glutathione (GSSG) (nmol/g Hb)	11.5 ± 0.56	14.21 ± 1.5^{+}	13.42 ± 2.35	12.85 ± 1.65
Glutathione redox ratio (GSSG/GSH)	0.15 ± 0.01	0.19 ± 0.02^{++}	0.17 ± 0.03	0.17 ± 0.02
Plasma values				
Hemoglobin metabolites (oxyHb+metHb+ hemichrome) (μmol/L)	10.4 ± 0.71	9.54 ± 1.14	11.66 ± 1.23*	10.39 ± 0.91$^{\#\#}$
Bilirubin (μmol/L)	12.4 ± 0.94	12.35 ± 1.39	17.01 ± 1.72**	11.81 ± 0.85$^{\#\#\#}$
FOX (IU/L)	0.59 ± 0.01	0.89 ± 0.03^{++}	0.96 ± 0.04*	0.88 ± 0.04$^{\#\#}$
Homocysteine (μmol/L)	12.4 ± 1.16	35.1 ± 4.41^{+++}	25.9 ± 3.03**	33.7 ± 3.63$^{\#}$

Tukey test * P<0.05; ** P<0.01 before vs. immediately after HD; # P<0.05; ## P<0.01; ### P<0.001 immediately after HD vs. 48 h after HD

t-test $^{+}$ P<0.05; $^{++}$ P<0.01; $^{+++}$ P<0.001 controls vs. dialyzed patients before HD.

The plasma Hb (9.54±1.14 before and 11.66±1.23 after HD, $P<0.05$), Bi (12.35±1.39 before and 17.01±1.72 after HD, $P<0.01$), and FOX (0.89±0.03 before and 0.96±0.04 after HD, $P<0.05$) levels increased significantly during HD, but had reverted to the original values by 48 h after HD (Table 4). During HD the homocysteine levels (35.1±4.41 before and 25.9±3.03 after HD, $P<0.01$) decreased significantly, but these levels in our patients were still significantly higher than in healthy controls (12.4±1.16, $P<0.001$) (Table 4). We did not find any significant HD-induced changes in the GSH and GSSG concentrations of HD patients either immediately or 48h later (Table 4).

Table 5. Comparison of some biochemical parameters in the whole blood and in the plasma of short-term and long-term HD patients (means±SEM)

	Before HD		Immediately after HD	
	Short-term (n=7)	Long-term (n=10)	Short-term (n=7)	Long-term (n=10)
Whole blood values				
Reduced glutathione (GSH) (μmol/g Hb)	7.76 ± 0.43	7.24 ± 0.38	7.90 ± 0.44	7.54 ± 0.39
Oxidized glutathione (GSSG) (nmol/g Hb)	14.7 ± 3.38	14.0 ± 1.05	16.1 ± 5.19	11.2 ± 1.44
Glutathione redox ratio (GSSG/GSH)	0.18 ± 0.04	0.20 ± 0.02	0.19 ± 0.06	0.15 ± 0.02
Plasma values				
Hemoglobin metabolites (μmol/L) (oxyHb+metHb+hemichrome)	8.49 ± 1.76	10.2 ± 1.53	9.04 ± 1.45	13.4 ± 1.65
Bilirubin (μmol/L)	10.7 ± 1.17	13.4 ± 2.21	13.4 ± 1.25	19.5 ± 2.56*
Ceruloplasmin ferroxidase (IU/L)	0.89 ± 0.04	0.88 ± 0.04	0.96 ± 0.05	0.96 ± 0.06
Homocysteine (μmol/L)	29.3 ± 6.88	39.5 ± 11.0	20.2 ± 4.74*	30.3 ± 8.50*

t-test * P<0.05 before HD vs. immediately after HD

The biochemical parameters in the short-term and long-term HD patients before and after HD are presented in Table 5. Bi levels were significantly higher ($p<0.05$) immediately after HD in long-term HD patients than that of short-term HD patients. Homocystein levels of long-term HD patients were significantly lower before ($p<0.05$) and immediately after ($P<0.05$) HD than that of short-term HD patients. We did not observe any significant differences in the GSH, GSSG, GSSG/GSH and Hb levels between the two groups prior to and after HD. No correlation was found between the HO-1 expression, the measured biochemical parameters, and the HD adequacy (Kt/V).

To estimate the effects of HD on the different parameters, the ratios (after HD)/(before HD) of the measured metabolites and the HO-1 mRNA levels were correlated. Significant correlation were found between the change in HO-1 mRNA level and the changes in plasma Hb level (r=0.72, $P<0.001$) and plasma Bi level (r=0.71, $P<0.002$) (Fig. 12). We found no other significant relationship between the changes in the other measured oxidative stress markers.

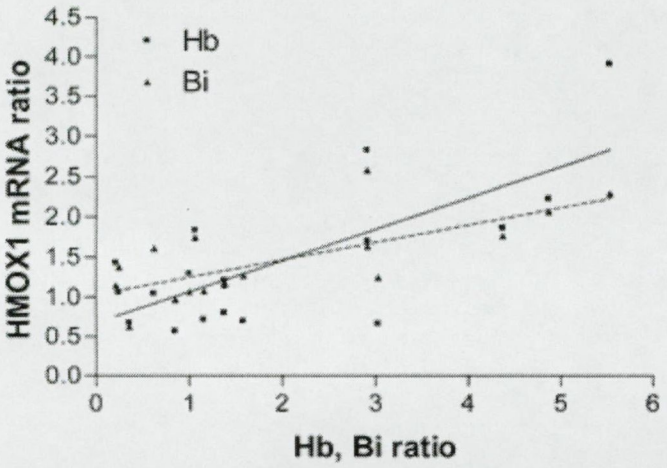

Fig. 12. Correlation of the HD-induced changes (ratio of values immediately after HD and before HD) in plasma hemoglobin (Hb) (r=0.72, $P<0.001$) and bilirubin (Bi) (r=0.71, $P<0.002$) levels with HO-1 mRNA

The patients exhibited different levels of HO-1 inducibility, depending on the duration of their HD program. The short-term HD patients (n=7) had a higher baseline mRNA expression, which remained roughly the same during HD (Fig. 13A) and decreased slightly 48 h after HD, but these changes were not significant.

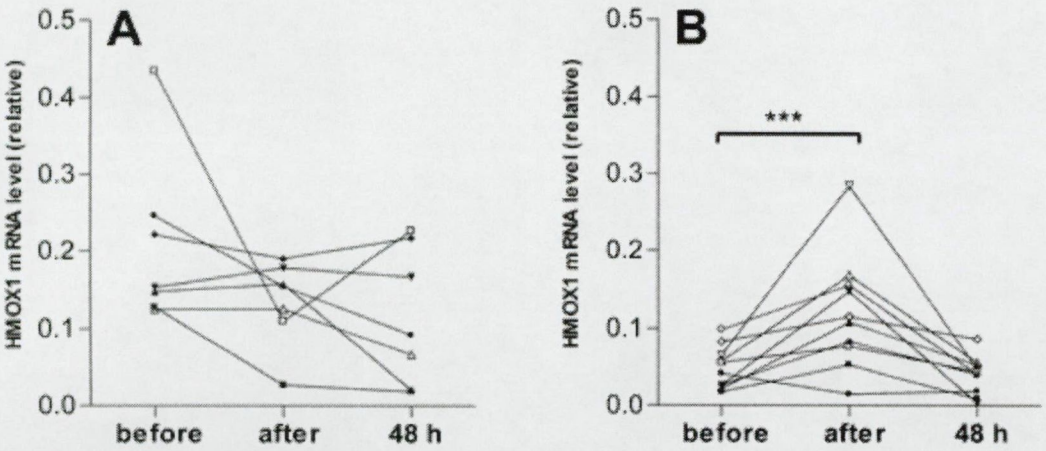

Fig. 13. HO-1 mRNA expression before, immediately after, and 48 h following HD in (**A**) short-term HD patients and (**B**) in long-term HD patients

The long-term HD patients (n=10) had a low baseline HO-1 mRNA expression, which underwent a one- to five-fold increase immediately after HD, but which had returned to the original value by 48 h (Fig. 13B).

4. DISCUSSION

4.1. FISH analysis of the break point regions of the Costello syndrome patient

In conclusion, we have confirmed the translocation breakpoint of the patient with Costello syndrome on chromosome 1q25 and mapped it to a 109-kb region. The breakpoint on chromosome 22 was refined to q13.1, and a cosmid with an insert of 38 kb was found that spanned the breakpoint. Suri and Garrett [58] described a Costello patient with acoustic neurinoma and cataract that are both features of neurofibromatosis type 2 (NF2). Although the authors did not find a deletion or point mutation of the NF2 gene, located in 22q12.2, it has been suggested that the gene for Costello syndrome might be close to NF2. If the Costello gene is located in 22q13.1, an inversion might have happened in the Costello/NF2 patient that escaped detection by conventional cytogenetic analysis. Further molecular analyses of the breakpoints on chromosomes 1 and 22 are necessary to show whether a single gene or more genes are affected by the translocation. Mutation screening in future studies of patients with Costello syndrome who have a normal karyotype will show whether any of the genes located near/at the breakpoints identified in our studies is the causative gene, or one of the causative genes for this syndrome.

4.2. Choosing a method to measure HO-1 induction

Quantitation of nucleic acids has become an essential tool in molecular diagnostics. Despite the fact that a number of methods are available for this purpose the procedures involved are rather cumbersome and each of them has its advantages and disadvantages.

In hybridization methods like Northern blotting, the RNase protection assay and chip technology for detecting specific mRNAs, the reaction kinetics are easier to determine, but the sensitivity is not sufficient for most practical applications. In contrast, due to the amplifying effect, PCR-based methods are more sensitive. However, the kinetic of PCR is more complex and hence the use of PCR as a quantitative method is not straightforward.

In the past few years, there have been many publications dealing with the quantitation of PCR products. The first approaches were only semiquantitative and were based on limiting dilution of the analyte [59]. Other methods used external standard curves for quantitation [60]

or low-stringency PCR [61]. None of these approaches overcame the problem of inhibition of individual probes. As a consequence, the next generation focused on amplification reactions that were internally controlled, either by co-amplification of internal endogenous standards, such as housekeeping genes [62, 63], or by introduction of an artificial exogenous competitor fragment [64-66]. For detailed reviews, see Clementi et al. [67, 68].

Competitive PCR is a powerful tool for accurate quantification of low amount of DNA or RNA. It has several well established advantages over other methods for RNA quantitation utilizing RT-PCR [69-71]. The procedure relies on the co- reverse transcription and amplification of the sequence of interest with a serially diluted synthetic RNA fragment of known concentration (competitor) using a single set of primers [72, 73]. In particular, being the quantification procedure based on the calculation of the ratio between the amounts of competitor and target products, the technique is unaffected by the overall yield of either the RT or PCR steps, allows the experimenter to reach the plateau of amplification, and is insensitive to the formation of aspecific products.

The limiting step in the development of a competitive RT-PCR assay, however, is represented by the construction of competitor RNA templates. For this purpose we used a PCR based in vitro mutagenesis method [52], which does not require cloning of template DNA, and other labor intensive methods using restriction endonuclease and ligation techniques [74-77]. By using this method, since the competitor RNAs differ in size from the targets, the resulting amplification products can be simply resolved by gel electrophoresis and detected by ethidium bromide staining, avoiding the need for complex separation or internal hybridization procedures, in contrast to other competitive methods [78, 79].

The other problem using an externally created competitor is that although it is capable of absolute measurement, in real world usage it can be only applied when the amount of the analyzed sample is exactly known. This difficulty is usually overcome by using the RNA of a housekeeping gene as external control in other methods [62, 63]. This approach has its own difficulties however. The PCR amplification of the two different primers, which amplifies the external control and the target sequence usually have different non-linear amplification characteristic. Furthermore in this duplex PCR the primer-primer formation, primer-template interaction may further complicate the measurements and requires non-linear calibration curves and complex software for the data analysis. To decrease the above mentioned effects the kinetics obtained during the exponential phase of PCR are used for quantification. For these measurements currently the real time PCR methods using fluorescent detection are

suitable as the conventional methods (staining with ethidium bromide and gel electrophoresis) are not sensitive enough.

Overall, the competitive RT-PCR is an affordable robust technique which does not need special RNA purification and unaffected by the yield of either the RT or PCR steps. On the negative side, it is labor intensive and time consuming, thus limiting the numbers of samples which can be analyzed at a given time. LightCycler RT-PCR is costly and very susceptible to even traces of inhibitors, but it allows high-throughput processing of samples.

Free heme is a substrate and inductor of its catabolizing enzyme, HO-1, which is also expressed in the lympho-, mono- and granulocytes in blood [80]. This let us set up a convenient methodology for our measurements on blood. HO-1 is transcriptionally induced and we could therefore apply a sensitive competitive RT-PCR method to measure the increased copy number of HMOX1 mRNA instead of measuring HO-1 protein by immunoassay. Compared to immunoassay methods RNA copy number based methods are more sensitive due to the amplifying chain reaction of PCR. The method was sensitive enough for the quantitative analysis of HMOX1 mRNA separated from 100 µl of whole blood. In our experiments the target tissue was blood therefore we could use the white blood cell count to quantify the samples and measure HMOX1 mRNA copy number per white blood cell.

4.3. HO-1 expression in mature and premature neonates

Heme functions as a double-edged sword. In moderate quantities and bound to protein, it forms an essential element for various biological processes, but when unleashed in large amounts, it can become toxic by mediating oxidative stress and inflammation. The effect of this free heme on the vascular system is determined by extracellular factors, such as hemoglobin/heme-binding proteins, haptoglobin, albumin, and hemopexin, and intracellular factors, including heme oxygenases and ferritin. Heme oxygenase enzyme activity results in the degradation of heme and the production of iron, carbon monoxide, and biliverdin. All these heme-degradation products are potentially toxic, but may also provide strong cytoprotection, depending on the generated amounts and the microenvironment. Approximately 5% of newborns suffer from neonatal jaundice, or hyperbilirubinemia. If the bilirubin levels become dangerously high, bilirubin passes through the blood-brain barrier and can cause neuronal damage associated with kernicterus [81]. The most common treatment for

hyperbilirubinemia is phototherapy, in which the jaundiced infant is exposed to blue light. The therapeutic effect is mediated by photoisomerization of unconjugated bilirubin, resulting in more polar and readily excretable photoisomers [82]. Recently, alternative treatment with competitive inhibitors of HO activity, such as stannic mesoporphyrin (single dose of 6 μmol/kg), has shown to prevent and to reverse bilirubinemia [83, 84].

Under normal physiological conditions, most cells express low or undetectable levels of HO-1 protein [85]. In our study, the elevated HO-1 expression level immediately after birth is an indicator of oxidative stress in both mature and premature newborns. As the HO-1 levels increased during the following days (Fig. 10.) we can conclude that HO-1 is inducible in this early stage in both mature and premature neonates. The fact that the induction of HO-1 mRNA and its maximum precede the maximal bilirubin levels (Fig. 11.) demonstrates that HO-1 is functional and cleaves free heme to biliverdin, CO and Fe^{2+}. Due to the fact that neonates bellow 32 weeks of gestation have a very immature antioxidant enzymatic activity same oxidative stress can lead to a higher stress response. They are also more susceptible to oxidative injury caused by the oxidative stress. Therefore we think that the earlier up-regulation of HO-1 expression of premature neonates could be perhaps attributed to the oxidative stress caused by the extra O_2 administration in these patients. However we found no significant correlation between HO-1 expression and the FiO_2 values in the examined patients. It could be because of the statistically low number of patients on extra O_2 therapy and that O_2 was supplied only to reach 90% saturation thus the generated oxidative stress must had been quite modest in these patients compared to the oxidative effect of liberated free heme. By our data inducibility of HO-1 does not depend on the gestational age.

It has been shown that in species in which hemolysis takes place post parturition, the activity of HO is enhanced in the early newborn period [86]. Our results in human newborns confirm this finding. It is also suggested that HO-1 activity is required for iron reutilization in mammals [35] for the prevention of abnormal iron accumulation in hepatic and renal cells, which otherwise contributes to oxidative damage, tissue injury and chronic inflammation. HMOX1-deficient adult mice developed an anemia associated with abnormally low serum iron levels, yet accumulated hepatic and renal iron that contributed to macromolecular oxidative damage, tissue injury, and chronic inflammation. These results indicate that HMOX1 has an important recycling role by facilitating the release of iron from hepatic and renal cells. Accordingly, our results underlines that the early inducibility of HO-1 even in

premature neonates is essential to avoid iron metabolic disorders and the injury caused by oxidative stress.

The one HMOX1 deficient patient suffered from growth failure, anemia, tissue iron deposition, lymphadenopathy, leukocytosis, and increased sensitivity to oxidant injury. He ultimately succumbed to a premature death [87]. In an animal model of HO-1 deficiency, mice lacking the gene frequently die *in utero*, and those surviving to term display a phenotype similar to the HO-1-deficient boy [35]. Clearly, HO-1 is necessary to the survival of organisms. In our study both the mature and premature neonates we investigated were free from any organ manifestation of oxidative stress. In spite of the fact that many enzymes shows enzyme immaturity in premature neonates the two groups of patients did not exhibit differences in HO-1 expression pattern or inducibility. We therefore concluded that HO-1 plays a crucial role in the early physiological adaptation of both mature and premature neonates.

Oxygen radical injury is a common pathogenic mechanism in a number of neonatal diseases, including idiopathic respiratory distress syndrome, retinopathy of prematurity, bronchopulmonary dysplasia, subependymal and intraventricular hemorrhage and necrotizing enterocolitis [12, 88]. These disorders display a higher incidence in preterm infants with deficient antioxidant protective systems [89]. Our study indicates that premature neonates without any organ manifestation of oxygen radical injury are prepared to handle the released heme by the induction of the HO-1 system during neonatal adaptation. The question arises of whether the disturbance of HO-1 inducibility plays a role in premature newborns with "oxygen radical disease of prematurity".

4.4. HO-1 expression in young hemodialysed uremic patients

Oxidized free hemoglobin in the plasma mediates low-density lipoprotein oxidation and provides the endothelium with heme, which greatly enhances the oxidant-mediated cell injury, resulting in the endothelial dysfunction usually present in HD-treated uremic patients [35, 90]. Besides the oxidant insult of HD per se, a compromised erythrocyte defense mechanism against free oxygen radicals has been recognized to contribute to the HD-induced oxidative hemolysis in uremic patients [91, 92]. However, after heme-induced sensitization, the endothelium responds to chronic heme exposure by up regulating a group of stress proteins to maintain the structural and functional integrity of the cells [93]. Hb metabolism plays an

important role in HD mediated endothelial injury. The changes in Hb metabolism in uremic patients on HD could also contribute to the accelerated progression of atherosclerosis.

In our study the increased levels of Hb in the plasma indicated a mechanical and oxidative hemolysis during HD (Table 4). The consecutive increase in Bi is a result of the functional HO eliminating free heme and protecting the arterial endothelium from oxidative stress. The catabolic cleavage of heme by HO-1 results in biliverdin, carbon monoxide, and Fe^{2+}, which in turn up regulates the FOX system. The FOX activity in the HD patients (0.89±0.03 before HD) was significantly ($P<0.01$) higher than that in the controls (0.59±0.01), possibly as a result of the oxidative stress in the HD patients (Table 4). During HD, FOX activity increased significantly (0.89±0.03 before and 0.96±0.04 after HD, $P<0.05$) due to the oxidative stress caused by HD.

In the HD patients, the ratio GSSG/GSH was higher than in controls, indicating that the oxidative stress in uremic HD patients. However, significant changes were not observed during HD, suggesting that the free heme was effectively catabolized by the HO. The rapid up-regulation of HO-1, and the consecutive up-regulation of the FOX system eliminates the free heme and stops the further generation of free radicals.

The homocysteine concentration was significantly higher in the HD patients than controls. Such an increased homocysteine level is an independent risk factor for vascular disease, a sign of progressing atherosclerosis [94]. During HD, homocysteine was dialyzed out from the plasma, the level in the patients therefore decreased significantly.

This study, which monitored the alteration in the HD-associated oxidative stress after one HD session, revealed significant differences in HO-1 inducibility, depending on the duration of HD treatment. In those patients who had been on HD for a shorter duration, the baseline HO-1 mRNA expression was higher than in those undergoing long-term HD. In the short-term patients, the plasma Hb level did not increase significantly during one HD session, because of the already elevated HO-1 level, and HO-1 was not further induced. In the long-term HD patients, the baseline HO-1 mRNA expression was low and the HO-1 expression was up-regulated one- to five-fold during HD, due to the ensuing hemolysis.

Our study measured the induction of the HO-1 mRNA level, which in turn leads to elevated HO-1 levels. However, HO-1 activity can be different before and after HD because of the clearance of toxic metabolites from the plasma by HD. These toxic metabolites may inhibit HO-1 activity, resulting in an impaired cytoprotective capacity prior to HD.

As we observed a significant correlation between the changes in plasma Hb and HO-1

mRNA levels ($P<0.001$) and also between the changes in plasma Bi and HO-1 mRNA levels ($P<0.002$), but not between the baseline HO-1 expression and the various measured biochemical parameters, we concluded that the HO-1 mRNA induction during HD is due to the hemolysis that occurs, but the baseline HO-1 expression is modulated by other factors. These results are in accordance with a study where the effect of erythropoietin treatment on hemolysis and HO-1 mRNA levels was investigated [95] in HD patients. A previous study demonstrated that endurance exercise in humans is also followed by an increased HO-1 mRNA expression in the monocytes, leukocytes, and (less so) lymphocytes [80]. Our results relating to the HO-1 mRNA expression reveal differences in short- and long-term HD patients, very similar to those reported in that study. In untrained subjects at rest, the HO-1 mRNA exhibited a higher baseline expression than in athletes [80]. It was suggested that the down-regulation of the baseline expression of HO-1 reflect an adaptation mechanism to regular exercise training. The corresponding change in our patients could be attributed to a mechanism of adaptation to the regularly occurring stress during HD.

Experimental results suggested that a permanent up-regulation of HO-1 may afford protection against atherosclerosis, as HO-1 inhibits atherosclerotic lesion formation in low-density lipoprotein receptor knockout mice [96]. It was also observed that cellular resistance to oxidative stress correlates positively with levels of HO-1 expression. In fact, researchers using various *in vitro* or *in vivo* stress paradigms have found that experimental up-regulation of HO-1 by treatment with heme or hemoglobin affords protection against subsequent oxidative challenges [97-99]. Long-term HD patients are subject to a periodic (3 times a week) increase in free heme levels at the beginning of each HD sessions, as there is latency between the appearance of liberated heme and the transcriptional up-regulation of HO-1 expression. This short (1–2 h) periodic exposure to increased free heme could cause the oxidative damage of endothelium and accelerate atherosclerosis. The chronic down-regulation of the baseline HO-1 expression in long-term HD patients may contribute to the progression of atherosclerosis.

5. SUMMARY

We confirmed the translocation breakpoint of the patient with Costello syndrome on chromosome 1q25 and mapped it to a 109-kb region. The breakpoint on chromosome 22 was refined to q13.1, and a cosmid with an insert of 38 kb was found that spanned the breakpoint.

We established a molecular genetic approach to measure directly the HMOX1 mRNA expression. This was convenient because:

- HO-1 is transcriptionally regulated through the copy number of HMOX1 mRNA
- HO-1 is expressed in white blood cells thus sample collection was easy
- the method was suitable to analyze even low amount (100 µl) of samples
- the amount of mRNA could be expressed in reference with white blood cell count thus directly showing us mRNA copy number per cells
- the method is robust and insensitive of inhibitors of either the RT or the PCR amplification steps
- inexpensive, the whole procedure can be carried out with conventional non real time PCR instrument

The drawback of the method was:

- the competitor fragment was difficult to create
- the procedure is labour-intensive

In our experiments with HO-1 expression in healthy mature and premature we found that level of HO-1 expression and its induction profile are similar in both mature and premature neonates during the first week after birth. We also showed that HO-1 is functional in both mature and premature neonates because the induction of HO-1 was followed by the increase of the bilirubin levels. Thus in healthy neonates HO-1 does not play a role in the

transitory adaptation disturbances however it has an important role in the physiological adaptation process. Our study revealed the importance that further analysis is needed to analyze the HO-1 expression in neonates with organic manifestation of oxidative injury.

In HD patients we showed that there is a significant difference in the HO-1 expression pattern between the patients depending on the duration of HD treatment. Short-term HD patients have an elevated HO-1 expression which may be contributed to an ongoing inflammation process. Long-term HD patients have a low base line HO-1 expression which was up regulated 1-5 fold during one single HD session. We also showed that the induction of HO-1 significantly correlated ($P<0.001$) with the occurring hemolysis and the liberated heme. We concluded that the periodical oxidative injury (three times a week) due to every HD sessions and the time delay between the occurring hemolysis and up-regulation of HO-1 could also contribute to the accelerated atherosclerosis rate in long-term HD patients.

6. ACKNOWLEDGEMENT

I would like to thank Prof. Dr. Sándor Túri, Chairman of the Department of Pediatric, University of Szeged for the encouragement, scientific guidance and opportunity to work at the institute and Dr. Emőke Endreffy, the Head of the Genetic Laboratory of the Department of Pediatric, University of Szeged for her scientific guidance, and continuous support. I would also like to thank Dr. Ilona Németh and Dr. Eszter Karg, Department of Pediatric, University of Szeged for their scientific guidance and encouragement.

I would also like to thank Dr. Márta Katona, Head of the PIC at the Department of Pediatric, University of Szeged and Dr. Hajnalka Orvos, Department of Gynecology, University of Szeged for the help and opportunity to collect samples from the neonate patients. I whish to acknowledge the practical help of Péter Ugocsai and Ildikó Farkas medical students in the laboratory experiments and sample collection.

I would like to thank Prof. Andreas Gal, Chairman of the Institut für Humangenetik, UKHE, Hamburg for his scientific guidance and the opportunity to work at the institute. I would also like to thank my supervisor Kerstin Kutsche, Ph.D. Institut für Humangenetik UKHE, Hamburg for introducing me into the molecular genetics methods and for her help and scientific guidance in the Costello syndrome project. I would also like to thank to Margarita Stefanova and Barbara Schröder for their help in the FISH techniques and Kirsten von Hadeln and Karin Ziegler for cytogenetic analysis.

The positional cloning studies were sponsored by Deutsche Forschungsgemeinschaft; Grant number: GRK336. The HO-1 expression studies were supported by OTKA grant 022562, FKFP grant 0588/2000 and ETT grants 46406 and 46506/2000.

7. REFERENCES

1. Costello JM. A new syndrome: mental subnormality and nasal papillomata. Aust Paediatr J 1977: 13(2): 114-8.

2. Costello JM. A new syndrome. NZ Med J 1971: 74: 397.

3. Lurie IW. Genetics of the Costello syndrome. Am J Med Genet 1994: 52(3): 358-9.

4. Berberich MS, Carey JC, Hall BD. Resolution of the perinatal and infantile failure to thrive in a new autosomal recessive syndrome with the phenotype of a storage disorder and furrowing of palmar creases. Proc. Greenwood Genet. Center 1991: 10: 78.

5. Zampino G, Mastroiacovo P, Ricci R et al. Costello syndrome: further clinical delineation, natural history, genetic definition, and nosology. Am J Med Genet 1993: 47(2): 176-83.

6. Borochowitz Z, Pavone L, Mazor G et al. New multiple congenital anomalies: mental retardation syndrome (MCA/MR) with facio-cutaneous-skeletal involvement. Am J Med Genet 1992: 43(4): 678-85.

7. Johnson JP, Golabi M, Norton ME et al. Costello syndrome: phenotype, natural history, differential diagnosis, and possible cause. J Pediatr 1998: 133(3): 441-8.

8. Tartaglia M, Cotter PD, Zampino G et al. Exclusion of PTPN11 mutations in Costello syndrome: further evidence for distinct genetic etiologies for Noonan, cardio-facio-cutaneous and Costello syndromes. Clin Genet 2003: 63(5): 423-6.

9. Ion A, Tartaglia M, Song X et al. Absence of PTPN11 mutations in 28 cases of cardiofaciocutaneous (CFC) syndrome. Hum Genet 2002: 111(4-5): 421-7.

10. Czeizel AE, Timar L. Hungarian case with Costello syndrome and translocation t(1,22). Am J Med Genet 1995: 57(3): 501-3.

11. McCarthy K, Bhogal M, Nardi M et al. Pathogenic factors in bronchopulmonary dysplasia. Pediatr Res 1984: 18(5): 483-8.

12. Rogers S, Witz G, Anwar M et al. Antioxidant capacity and oxygen radical diseases in the preterm newborn. Arch Pediatr Adolesc Med 2000: 154(6): 544-8.

13. Balla G, Vercellotti GM, Muller-Eberhard U et al. Exposure of endothelial cells to free heme potentiates damage mediated by granulocytes and toxic oxygen species. Lab Invest 1991: 64(5): 648-55.

14. Jeney V, Balla J, Yachie A et al. Pro-oxidant and cytotoxic effects of circulating heme. Blood 2002: 100(3): 879-87.

15. Foley RN, Parfrey PS, Sarnak MJ. Epidemiology of cardiovascular disease in chronic renal disease. J Am Soc Nephrol 1998: 9(12 Suppl): S16-23.

16. Rocco MV, Yan G, Gassman J et al. Comparison of causes of death using HEMO Study and HCFA end-stage renal disease death notification classification systems. The National Institutes of Health-funded Hemodialysis. Health Care Financing Administration. Am J Kidney Dis 2002: 39(1): 146-53.

17. Rattazzi M, Puato M, Faggin E et al. New markers of accelerated atherosclerosis in end-stage renal disease. J Nephrol 2003: 16(1): 11-20.

18. Clermont G, Lecour S, Lahet J et al. Alteration in plasma antioxidant capacities in chronic renal failure and hemodialysis patients: a possible explanation for the increased cardiovascular risk in these patients. Cardiovasc Res 2000: 47(3): 618-23.

19. Graham IM, Daly LE, Refsum HM et al. Plasma homocysteine as a risk factor for vascular disease. The European Concerted Action Project. Jama 1997: 277(22): 1775-81.

20. Durak I, Kacmaz M, Elgun S et al. Oxidative stress in patients with chronic renal failure: effects of hemodialysis. Med Princ Pract 2004: 13(2): 84-7.

21. Loughrey CM, Young IS, Lightbody JH et al. Oxidative stress in haemodialysis. Qjm 1994: 87(11): 679-83.

22. Maines MD. Heme oxygenase: function, multiplicity, regulatory mechanisms, and clinical applications. Faseb J 1988: 2(10): 2557-68.

23. Stocker R, Yamamoto Y, McDonagh AF et al. Bilirubin is an antioxidant of possible physiological importance. Science 1987: 235(4792): 1043-6.

24. Marilena G. New physiological importance of two classic residual products: carbon monoxide and bilirubin. Biochem Mol Med 1997: 61(2): 136-42.

25. Tomaro ML, Batlle AM. Bilirubin: its role in cytoprotection against oxidative stress. Int J Biochem Cell Biol 2002: 34(3): 216-20.

26. Baranano DE, Rao M, Ferris CD et al. Biliverdin reductase: a major physiologic cytoprotectant. Proc Natl Acad Sci U S A 2002: 99(25): 16093-8.

27. Tyrrell RM, Basu-Modak S. Transient enhancement of heme oxygenase 1 mRNA accumulation: a marker of oxidative stress to eukaryotic cells. Methods Enzymol 1994: 234: 224-35.

28. Stocker R. Induction of haem oxygenase as a defence against oxidative stress. Free Radic Res Commun 1990: 9(2): 101-12.

29. Nath KA, Haggard JJ, Croatt AJ et al. The indispensability of heme oxygenase-1 in protecting against acute heme protein-induced toxicity in vivo. Am J Pathol 2000: 156(5): 1527-35.

30. Wang LJ, Lee TS, Lee FY et al. Expression of heme oxygenase-1 in atherosclerotic lesions. Am J Pathol 1998: 152(3): 711-20.

31. Keyse SM, Tyrrell RM. Heme oxygenase is the major 32-kDa stress protein induced in human skin fibroblasts by UVA radiation, hydrogen peroxide, and sodium arsenite. Proc Natl Acad Sci U S A 1989: 86(1): 99-103.

32. Kutty RK, Nagineni CN, Kutty G et al. Increased expression of heme oxygenase-1 in human retinal pigment epithelial cells by transforming growth factor-beta. J Cell Physiol 1994: 159(2): 371-8.

33. Kutty RK, Kutty G, Rodriguez IR et al. Chromosomal localization of the human heme oxygenase genes: heme oxygenase-1 (HMOX1) maps to chromosome 22q12 and heme oxygenase-2 (HMOX2) maps to chromosome 16p13.3. Genomics 1994: 20(3): 513-6.

34. Seroussi E, Kedra D, Kost-Alimova M et al. TOM1 genes map to human chromosome 22q13.1 and mouse chromosome 8C1 and encode proteins similar to the endosomal proteins HGS and STAM. Genomics 1999: 57(3): 380-8.

35. Poss KD, Tonegawa S. Heme oxygenase 1 is required for mammalian iron reutilization. Proc Natl Acad Sci U S A 1997: 94(20): 10919-24.

36. Wagener FADTG, van Beurden HE, von den Hoff JW et al. The heme-heme oxygenase system: a molecular switch in wound healing. Blood 2002: 102: 521-528.

37. Yachie A, Niida Y, Wada T et al. Oxidative stress causes enhanced endothelial cell injury in human heme oxygenase-1 deficiency. Journal of Clinical Invest 1999: 103: 129-135.

38. Ryter SW, Tyrrell RM. The heme synthesis and degradation pathways: role in oxidant sensitivity. Heme oxygenase has both pro- and antioxidant properties. Free Radic Biol Med 2000: 28(2): 289-309.

39. Suttner DM, Dennery PA. Reversal of HO-1 related cytoprotection with increased expression is due to reactive iron. Faseb J 1999: 13(13): 1800-9.

40. Lamb NJ, Quinlan GJ, Mumby S et al. Haem oxygenase shows pro-oxidant activity in microsomal and cellular systems: implications for the release of low-molecular-mass iron. Biochem J 1999: 344 Pt 1: 153-8.

41. Dennery PA, Visner G, Weng YH et al. Resistance to hyperoxia with heme oxygenase-1 disruption: role of iron. Free Radic Biol Med 2003: 34(1): 124-33.

42. Abraham NG, Lavrovsky Y, Schwartzman ML et al. Transfection of the human heme oxygenase gene into rabbit coronary microvessel endothelial cells: protective effect against heme and hemoglobin toxicity. Proc Natl Acad Sci U S A 1995: 92(15): 6798-802.

43. Dennery PA, Sridhar KJ, Lee CS et al. Heme oxygenase-mediated resistance to oxygen toxicity in hamster fibroblasts. J Biol Chem 1997: 272(23): 14937-42.

44. Rogers B, Yakopson V, Teng ZP et al. Heme oxygenase-2 knockout neurons are less vulnerable to hemoglobin toxicity. Free Radic Biol Med 2003: 35(8): 872-81.

45. Yamada N, Yamaya M, Okinaga S et al. Microsatellite polymorphism in the heme oxygenase-1 gene promoter is associated with susceptibility to emphysema. Am J Hum Genet 2000: 66(1): 187-95.

46. da Silva JL, Morishita T, Escalante B et al. Dual role of heme oxygenase in epithelial cell injury: contrasting effects of short-term and long-term exposure to oxidant stress. J Lab Clin Med 1996: 128(3): 290-6.

47. Hebbel RP, Eaton JW. Pathobiology of heme interaction with the erythrocyte membrane. Semin Hematol 1989: 26(2): 136-49.

48. Burke DT, Carle GF, Olson MV. Cloning of large segments of exogenous DNA into yeast by means of artificial chromosome vectors. 1987. Biotechnology 1992: 24: 172-8.

49. Philippsen P, Stotz A, Scherf C. DNA of Saccharomyces cerevisiae. Methods Enzymol 1991: 194: 169-82.

50. Sambrook J, Fritsch E, Maniatis T. *Molecular Cloning*, in *A Laboratory Manual*. 1989, Cold Spring Harbor Laboratory: New York.

51. Kutsche K, Glauner E, Knauf S et al. Cloning and characterization of the breakpoint regions of a chromosome 11;18 translocation in a patient with hamartoma of the retinal pigment epithelium. Cytogenet Cell Genet 2000: 91(1-4): 141-7.

52. Waha A, Watzka M, Koch A et al. A rapid and sensitive protocol for competitive reverse transcriptase (cRT) PCR analysis of cellular genes. Brain Pathol 1998: 8(1): 13-8.

53. Jacobsen J, Wennberg RP. Determination of unbound bilirubin in the serum of newborns. Clin Chem 1974: 20(7): 783.

54. Johnson DA, Osaki S, Frieden E. A micromethod for the determination of ferroxidase (ceruloplasmin) in human serums. Clin Chem 1967: 13(2): 142-50.

55. Feussner A, Rolinski B, Weiss N et al. Determination of total homocysteine in human plasma by isocratic high-performance liquid chromatography. Eur J Clin Chem Clin Biochem 1997: 35(9): 687-91.

56. Nemeth I, Boda D. Blood glutathione redox ratio as a parameter of oxidative stress in premature infants with IRDS. Free Radic Biol Med 1994: 16(3): 347-53.

57. Klaus MH, Fanaroff AA. Care of the High-Risk Neonate. 5 ed. Philadelphia: W.B. Saunders, 2001.

58. Suri M, Garrett C. Costello syndrome with acoustic neuroma and cataract. Is the Costello locus linked to neurofibromatosis type 2 on 22q? Clin Dysmorphol 1998: 7(2): 149-51.

59. Simmonds P, McOmish F, Yap PL et al. Sequence variability in the 5' non-coding region of hepatitis C virus: identification of a new virus type and restrictions on sequence diversity. J Gen Virol 1993: 74 (Pt 4): 661-8.

60. Whitby K, Garson JA. Optimisation and evaluation of a quantitative chemiluminescent polymerase chain reaction assay for hepatitis C virus RNA. J Virol Methods 1995: 51(1): 75-88.

61. Caballero OL, Villa LL, Simpson AJ. Low stringency-PCR (LS-PCR) allows entirely internally standardized DNA quantitation. Nucleic Acids Res 1995: 23(1): 192-3.

62. Chelly J, Montarras D, Pinset C et al. Quantitative estimation of minor mRNAs by cDNA-polymerase chain reaction. Application to dystrophin mRNA in cultured myogenic and brain cells. Eur J Biochem 1990: 187(3): 691-8.

63. Mallet F, Hebrard C, Livrozet JM et al. Quantitation of human immunodeficiency virus type 1 DNA by two PCR procedures coupled with enzyme-linked oligosorbent assay. J Clin Microbiol 1995: 33(12): 3201-8.

64. Wang AM, Doyle MV, Mark DF. Quantitation of mRNA by the polymerase chain reaction. Proc Natl Acad Sci U S A 1989: 86(24): 9717-21.

65. Gilliland G, Perrin S, Blanchard K et al. Analysis of cytokine mRNA and DNA: detection and quantitation by competitive polymerase chain reaction. Proc Natl Acad Sci U S A 1990: 87(7): 2725-9.

66. Besnard NC, Andre PM. Automated quantitative determination of hepatitis C virus viremia by reverse transcription-PCR. J Clin Microbiol 1994: 32(8): 1887-93.

67. Clementi M, Menzo S, Manzin A et al. Quantitative molecular methods in virology. Arch Virol 1995: 140(9): 1523-39.

68. Clementi M, Menzo S, Bagnarelli P et al. Quantitative PCR and RT-PCR in virology. PCR Methods Appl 1993: 2(3): 191-6.

69. Nedelman J, Heagerty P, Lawrence C. Quantitative PCR with internal controls. Comput Appl Biosci 1992: 8(1): 65-70.

70. Diviacco S, Norio P, Zentilin L et al. A novel procedure for quantitative polymerase chain reaction by coamplification of competitive templates. Gene 1992: 122(2): 313-20.

71. Siebert PD, Larrick JW. Competitive PCR. Nature 1992: 359(6395): 557-8.

72. Siebert PD, Larrick JW. PCR MIMICS: competitive DNA fragments for use as internal standards in quantitative PCR. Biotechniques 1993: 14(2): 244-9.

73. Lion T, Izraeli S, Henn T et al. Monitoring of residual disease in chronic myelogenous leukemia by quantitative polymerase chain reaction. Leukemia 1992: 6(6): 495-9.

74. Apostolakos MJ, Schuermann WH, Frampton MW et al. Measurement of gene expression by multiplex competitive polymerase chain reaction. Anal Biochem 1993: 213(2): 277-84.

75. Bolton MC, Dudhia J, Bayliss MT. Quantification of aggrecan and link-protein mRNA in human articular cartilage of different ages by competitive reverse transcriptase-PCR. Biochem J 1996: 319 (Pt 2): 489-98.

76. Paschen W, Djuricic B. Regional differences in the extent of RNA editing of the glutamate receptor subunits GluR2 and GluR6 in rat brain. J Neurosci Methods 1995: 56(1): 21-9.

77. Wu J, Sullivan DE, Gerber MA. Quantitative polymerase chain reaction for hepatitis B virus DNA. J Virol Methods 1994: 49(3): 331-41.

78. Becker-Andre M, Hahlbrock K. Absolute mRNA quantification using the polymerase chain reaction (PCR). A novel approach by a PCR aided transcript titration assay (PATTY). Nucleic Acids Res 1989: 17(22): 9437-46.

79. Henco K, Heibey M. Quantitative PCR: the determination of template copy numbers by temperature gradient gel electrophoresis (TGGE). Nucleic Acids Res 1990: 18(22): 6733-4.

80. Niess AM, Passek F, Lorenz I et al. Expression of the antioxidant stress protein heme oxygenase-1 (HO-1) in human leukocytes. Free Radic Biol Med 1999: 26(1-2): 184-92.

81. Gourley GR. Bilirubin metabolism and kernicterus. Adv Pediatr 1997: 44: 173-229.

82. McDonagh AF, Lightner DA. 'Like a shrivelled blood orange'--bilirubin, jaundice, and phototherapy. Pediatrics 1985: 75(3): 443-55.

83. Kappas A, Drummond GS, Valaes T. A single dose of Sn-mesoporphyrin prevents development of severe hyperbilirubinemia in glucose-6-phosphate dehydrogenase-deficient newborns. Pediatrics 2001: 108(1): 25-30.

84. Kappas A, Drummond GS, Henschke C et al. Direct comparison of Sn-mesoporphyrin, an inhibitor of bilirubin production, and phototherapy in controlling hyperbilirubinemia in term and near-term newborns. Pediatrics 1995: 95(4): 468-74.

85. Wagener FA, Volk HD, Willis D et al. Different faces of the heme-heme oxygenase system in inflammation. Pharmacol Rev 2003: 55(3): 551-71.

86. Maines MD, Kappas A. Metals as regulators of heme metabolism. Science 1977: 198(4323): 1215-21.

87. Yachie A, Niida Y, Wada T et al. Oxidative stress causes enhanced endothelial cell injury in human heme oxygenase-1 deficiency. J Clin Invest 1999: 103(1): 129-35.

88. Saugstad OD. Oxygen toxicity at birth: the pieces are put together. Pediatr Res 2003: 54(6): 789.

89. Sullivan JL. Iron, plasma antioxidants, and the 'oxygen radical disease of prematurity'. Am J Dis Child 1988: 142(12): 1341-4.

90. Libby P, Ridker PM, Maseri A. Inflammation and atherosclerosis. Circulation 2002: 105(9): 1135-43.

91. Turi S, Nemeth I, Vargha I et al. Erythrocyte defense mechanisms against free oxygen radicals in haemodialysed uraemic children. Pediatr Nephrol 1991: 5(2): 179-83.

92. Ceballos-Picot I, Witko-Sarsat V, Merad-Boudia M et al. Glutathione antioxidant system as a marker of oxidative stress in chronic renal failure. Free Radic Biol Med 1996: 21(6): 845-53.

93. Balla J, Balla G, Jeney V et al. Ferriporphyrins and endothelium: a 2-edged sword-promotion of oxidation and induction of cytoprotectants. Blood 2000: 95(11): 3442-50.

94. Yeun JY, Kaysen GA. C-reactive protein, oxidative stress, homocysteine, and troponin as inflammatory and metabolic predictors of atherosclerosis in ESRD. Curr Opin Nephrol Hypertens 2000: 9(6): 621-30.

95. Calo LA, Stanic L, Davis PA et al. Effect of epoetin on HO-1 mRNA level and plasma antioxidants in hemodialysis patients. Int J Clin Pharmacol Ther 2003: 41(5): 187-92.

96. Ishikawa K, Sugawara D, Wang X et al. Heme oxygenase-1 inhibits atherosclerotic lesion formation in ldl-receptor knockout mice. Circ Res 2001: 88(5): 506-12.

97. Balla J, Jacob HS, Balla G et al. Endothelial-cell heme uptake from heme proteins: induction of sensitization and desensitization to oxidant damage. Proc Natl Acad Sci U S A 1993: 90(20): 9285-9.

98. Otterbein L, Sylvester SL, Choi AM. Hemoglobin provides protection against lethal endotoxemia in rats: the role of heme oxygenase-1. Am J Respir Cell Mol Biol 1995: 13(5): 595-601.

99. Nath KA, Balla G, Vercellotti GM et al. Induction of heme oxygenase is a rapid, protective response in rhabdomyolysis in the rat. J Clin Invest 1992: 90(1): 267-70.

8. APPENDIX